Outstanding Academic Papers by Students
學生優秀作品

UNIVERSIDADE DE MACAU
UNIVERSITY OF MACAU

A 97.5% MAXIMUM EFFICIENCY, FAST RESPONSE, LOW VOLTAGE RIPPLE KY BOOST CONVERTER FOR PHOTOVOLTAIC APPLICATION

by

WEN HAIJIE

Final Year Project Report submitted in partial fulfillment

of the requirements for the Degree of

Bachelor of Science in Electrical and Computer Engineering

2016

Faculty of Science and Technology

University of Macau

Bachelor's Thesis (or Final Report of ECEB420 Design Project II)

In presenting this Final Report of Design Project II (ECEB420) in partial fulfillment of the requirements for a Bachelor's Degree at the University of Macau, I agree that the **UM Library** and **Faculty of Science and Technology (FST)** shall make its copies available strictly for internal circulation or inspection. No part of this thesis can be reproduced by any means (electronic, mechanical, visual, etc.) before the valid date (usually less than 3 years) limit listed below. Copying of this thesis before the valid date from other parties is allowable **only** under the prior written permission of the author(s).

Printed name: _____

Signature: _____

Student number: _____

Date: _____

Reliable Contact information (address, tel. no., email, etc.) of author:

_____

_____

_____

_____

Valid date until _____

DECLARATION

I declare that the project report here submitted is original except for the source materials explicitly acknowledged and that this report as a whole, or any part of this report has not been previously and concurrently submitted for any other degree or award at the University of Macau or other institutions.

I also acknowledge that I am aware of the Rules on Handling Student Academic Dishonesty and the Regulations of the Student Discipline of the University of Macau.

Signature   : _____(e-signature OK)

Name   : WEN HAIJIE

Student ID   : D-B3-2685-6

Date   : 12/05/2017

APPROVAL FOR SUBMISSION

This project report entitled "**A 97.5% MAXIMUM EFFICIENCY, FAST RESPONSE, LOW VOLTAGE RIPPLE KY CONVERTER FOR PHOTOVOLTAIC APPLICATION**" was prepared by [Student's Name] (St. No.) in partial fulfillment of the requirements for the degree of Bachelor of Science in Electrical and Computer Engineering at the University of Macau.

Endorsed by,

Signature   : _____

Supervisor   : Dr. Chi-Seng Lam

Co-Supervisor(s)   : Dr. Chi-Kong Wong, Mr. Wai-Hei Choi

ABSTRACT

This project is focused on DC-DC step-up converter called KY converter which is characterized as high efficiency, fast transient response and low voltage ripple. By previous literature review, it can be found power electronics' market size was continuously growing. Meanwhile, by statistic analyze the paper published in IEEE transaction on power electronics between 2015 and 2016, power converter was the most popular topic. Among different conversion type between DC and AC, DC-DC converter shows its highest interest by researchers. As the rapid development of consumer electronics, renewable energy and HVDC application, DC-DC converter has a foreseeable bright future to work on.

In this project, theoretical study and simulation analysis by PSCAD/EMTDC was done for the KY converter. Based on theory, an experimental prototype was built up for used in renewable energy application in proposed. It is implemented with digital signal processor TMS320F2812 to perform the function as PID controller for enhance system's performance in close loop control. From previous experimental result, proposed system can achieve power efficiency up to 97.5% (200V/5A output).

TABLE OF CONTENTS

CHAPTER 1: INTRODUCTION

1.1 GENERAL BACKGROUND

1.1.1 POWER ELECTRONICS

For most of the electronic devices, power converter is necessary for satisfy various operating voltage and frequency level of different components interconnected. A well-designed converter can perform higher efficiency and reduce the size which can reduce the overall cost. Through statistical analyses the papers published in IEEE transaction of power electronic, the research in the areas of Low and High power converter has been the most popular topics in 2015 and 2016.
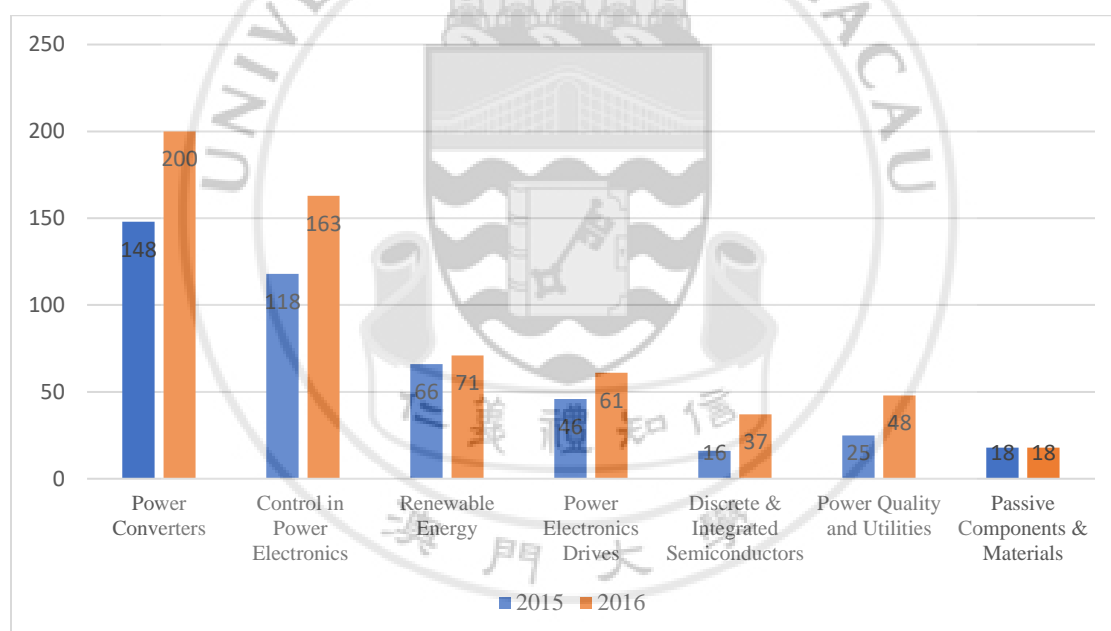
Figure 1.1.1 Number of paper published on IEEE in 2015 and 2016

Figure 1.1.1 shows the number of paper being published of most popular areas in power electronics in these two years. Within those 1409 published papers in these two years, 348 of them are sorted into power converters area. Near a quarter of advanced research on power electronic in past two years were focusing on power converters. Interleaved, multilevel, ZVS (zero voltage switching), hybrid are the words we can commonly find in the papers of converter. This reflected improvement on efficiency and reduce size are the greatest demand for converter design. Papers focused on

controls of power electronics took one fifth of total numbers. Generally, it includes control algorithms, control circuit design and small signal modelling. Renewable energy was the third most popular topic, which mainly focus on increase the conversion efficiency of adaptive control application. Like photovoltaic system and electric vehicle, MPPT (maximum power point tracking) technique is usually discussed. Except these popular fields, papers about power electronic drives, semiconductors in power electronics, power quality and up to 20 different fields often appear in publications.

Growing market can be considered as an importance driven factor for power electronic development. By the analysis of P&S Market Research, the global power electronics market was valued at $12,872.0 million in 2015 and is expected to witness a CAGR (compound annual growth rate) of 6.2% during 2016-2022 [1.1]. Based on technology, the power electronics market generated highest revenue from non-isolated DC-DC segment in 2015. Asia-Pacific contributed the largest revenues of global power electronics market global geographically. Yole Development also gave a similar picture of global power electronic market in their report. As shown in figure 1.1.2, the overall power electronics market size will keep growing in next five years.
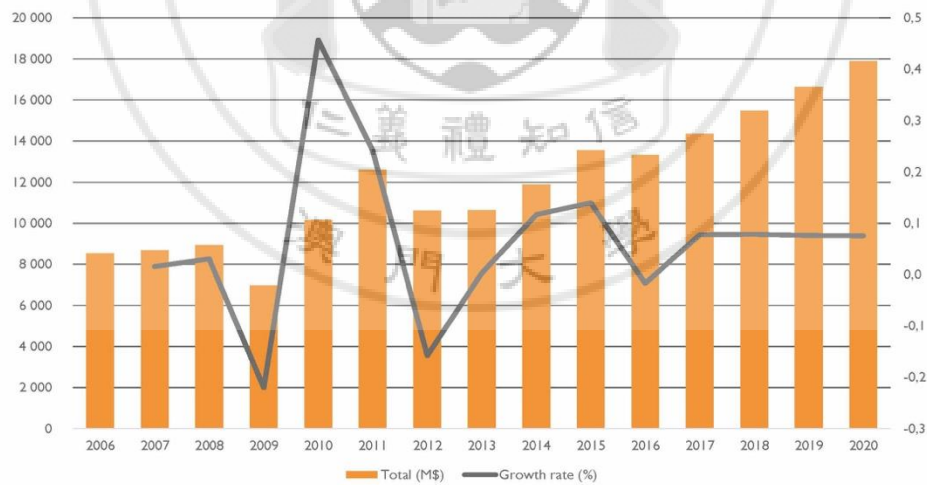
Figure 1.1.2 Power electronics market size between 2006 and 2020 [1.2]

1.1.2 POWER CONVERTER

Figure 1.1.1 shows power converter is the most interested area for researchers in both years. Moreover, quantity of paper published in this area was increasing. Within the papers discussed in power converters, 179 was discussing low power converters while 169 for high power, which means more than half were interested in low power and converter. Research preference can be further classified by different conversion type. Except papers interested in general modelling analysis and algorithm, DC-DC converter is a more popular of the research worldwide.
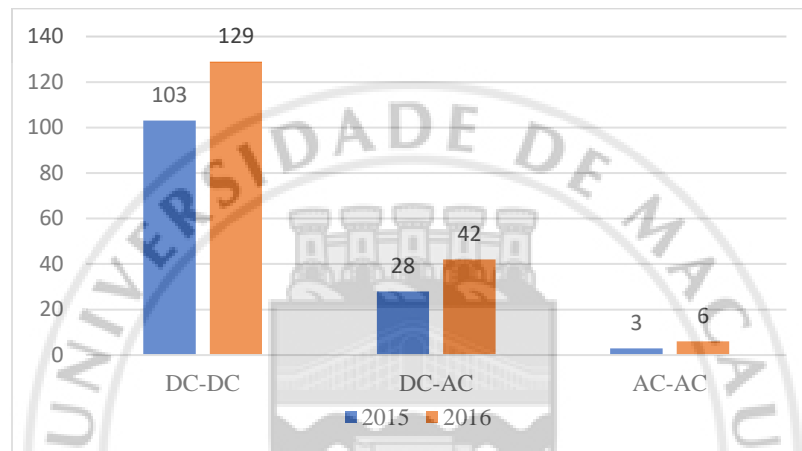
Figure 1.1.3 Different conversion type's distribution

Follow the developing trends of power electronics, market of converter also tends to grow in coming future. Total market size was 45 billion according to Yole Development's report published in 2013, while it is expected grow to 72 billion in 2020 [1.3].
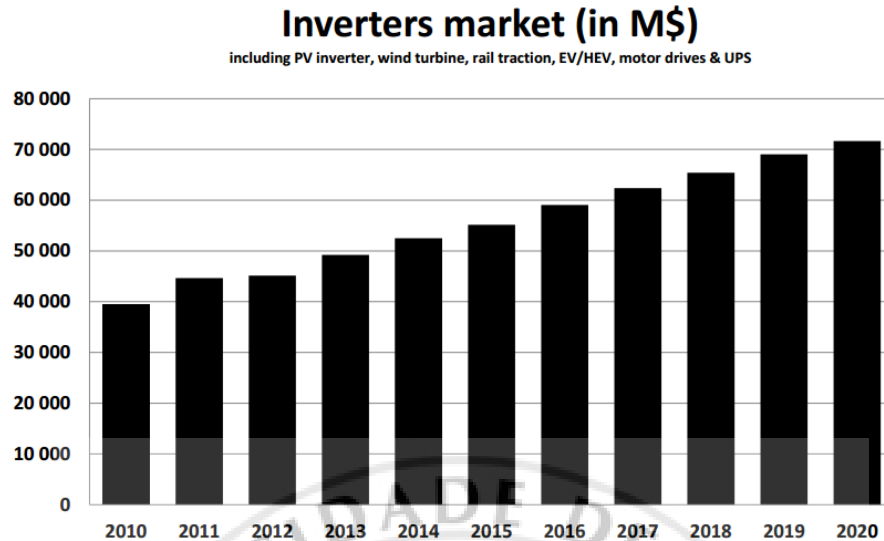
Figure 1.1.4 Inverter market trend between 2013 and 2020 [1.3]

1.2 DC-DC CONVERTER

1.2.1 FUNCTION OF DC-DC CONVERTER

Generally, it is a required component as energy link between different components if they are working in different voltage level. By connected to an unregulated constant voltage input, it can produce a regulated output voltage with possibly different voltage amplitude and polarity with input. Today, some analog components like RF and audio amplifier, or digital components like FGPAs and microprocessor employed in a variety of applications like telecommunications system, electric vehicles, laptops and smartphones. Inside the analog and digital components, DC-DC converter is necessary for satisfied different voltage level and maximize the power efficiency.

Figure 1.2.1 Applications of DC-DC converter

Functions of DC-DC converter can be divided into following categories [1.4]:

- Convert a DC input into an expected DC output.

- Regulate constant output with various load resistance.

- Reduce voltage ripple on the output below required level.

- Isolated input and output.

- Protect input source and power supply from electromagnetic interference.

1.2.2 TYPE OF DC-DC CONVERTER

Base of the output characteristic, fundamentally DC-DC converter can be divided into two categories: switching regulator and linear regulator. Switching regulators use power electronic switches in on and off states under the control of PWM signal, which means there will be no current flow in the input while switch is turned off. It is a discrete and nonlinear system. Conversely, linear regulator provides continuous current at both input and output of the converter. Different topologies widely used in these two categories will be introduced in the following parts. In comparison, their advantages and drawbacks can be found out.

1.2.2.1 SWITCHING REGULATOR

Basically, switching regulator provide higher conversion efficiency than linear regulator. Unlike linear regulator, switching components are periodically turned on and it means that the voltage

drop across its power path is minimal. There is almost no current go through when it is turned off. In general, there are three types of switching regulators: Buck (step-down) converter, boost (step-up) converter and buck-boost converter. Figure 1.2.2 to figure 1.2.4 show the basic structure of these topologies. These converters consist of input voltage source, capacitor, controlled power electronic switch, resistor and inductor. Among these components, inductor act as a relay. The switch is being operated with a duty ratio defined as a ratio between switch on time and the sum of on and off time. During turn on stage, the current in the inductor will increase to store energy; when the switched is turned off, inductor will release the stored energy. If the power losses (conduction loss, transistor switching loss, inductor core loss, etc.) is neglected, duty ratio also represents the relationship between input and output.
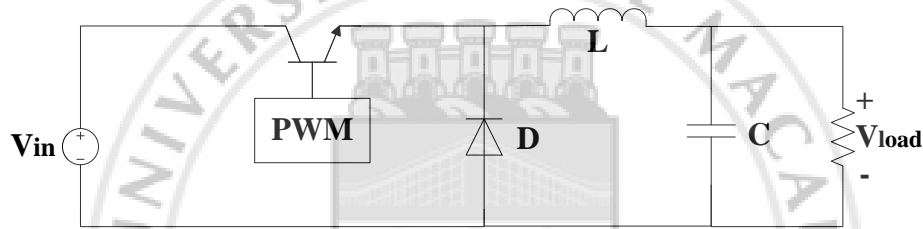

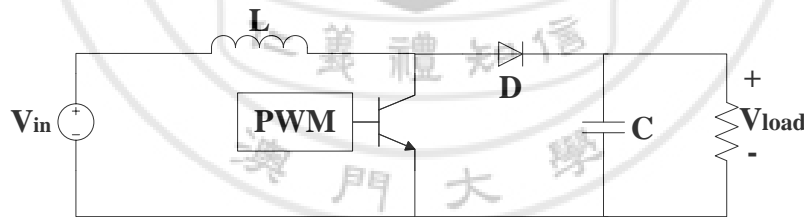
Figure 1.2.2 Basic structure of buck converter

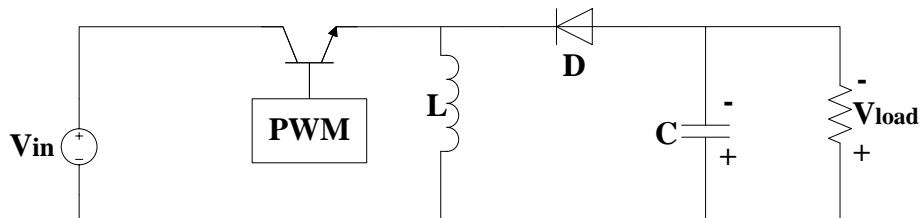Figure 1.2.3 Basic structure of boost converter

Figure 1.2.4 Basic structure of buck-boost converter

6

1.2.2.2 LINEAR REGULATOR

As a representative of linear regulator, low drop out (LDO) voltage regulator is widely used for many years which has a simple structure. LDO voltage regulator can generate a linear output from higher voltage input in relative lower cost. Figure 1.2.5 shows a series connected LDO voltage regulator with a resistive load and controllable switch. When the switch is open, voltage level on resistor is equals to input level while there will be not voltage on resistor if the switch is closed. The switch is controlled by duty ratio D. In LDO voltage regulator, duty ratio is also the ratio between input and output voltage. Besides, duty ratio of LDO voltage regulator almost equals to the efficiency η of converter. The efficiency can quickly estimate by equation (1.1). When the output level of LDO is much smaller than input, this regulator will dissipate lots of power and perform a low efficiency.

$$\mathrm{D}_{LDO} = \frac{V_{out}}{V_{out} + V_{in}} = \frac{P_{out}}{P_{out} + P_{loss}} = \eta_{LDO} \tag{1.1}$$
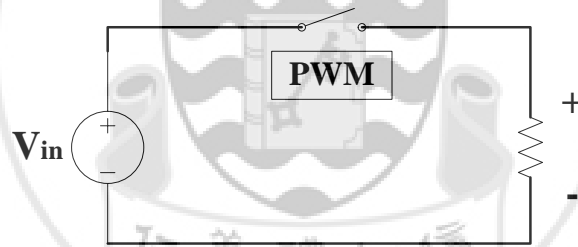
Figure 1.2.5 Basic structure of low drop out regulator

In addition, Cuk converter is also a common seen DC-DC converter which can provides continuous current at both input and output, but has a similar structure to the switching mode regulator that discussed. Like buck-boost converter, Cuk converter can both step-up and step-down input voltages but in same polarity. Essentially it can be obtained by cascading boost converter followed by buck converter. In the middle, there is an extra capacitor coupling the energy. However, the disadvantages of Cuk converter include more reactive components are required, also current stress on the switch component, diode and capacitor is higher.
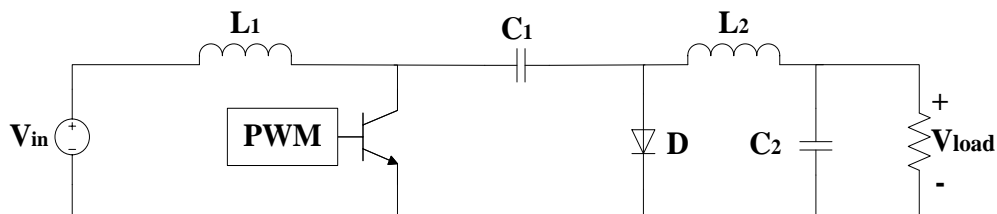
Figure 1.2.6 Basic structure of Cuk converter

1.2.3 COMPARISON OF DC-DC CONVERTER TOPOLOGIES

Table 1.2 shows a comparison of DC-DC converters been introduced from different considerations. Low drop out voltage regulator shows its advantages on simple structure and the smallest physical size. Consequently, it becomes a low-cost solution and easy to use. Meanwhile, LDO voltage regulator has less non-linear components which let the output ripple become very low. It makes it become appreciable for noise-sensitive applications like communication system. The major disadvantages of this topology are high power loss and limited output level. Only for low dropout applications (output level close to input), efficiency can become higher. Cuk converter is also a common linear regulator which can provide output voltage either higher or lower than input level in same polarity. However, its cost is higher since more components used.

	LDO Regulator	Buck Converter	Boost Converter	Buck-Boost Converter	Cuk Converter
Efficiency	Bad	Good	Good	Good	Good
Complexity	Low	Medium	Medium	Medium	High
Cost	Low	Medium	Medium	Medium	High
Output Ripple	Low	Medium	Medium	Medium	Medium
Load Ability	Bad	Medium	Medium	Good	Good
Size	Small	Medium	Medium	Medium	Big
Output Range	Small	Medium	Medium	Large	Large

Table 1.2 Comparison of general DC-DC converter topologies

In comparison, due to various components used especially inductor in the circuit, switching regulators normally has highest complexity and biggest size. Although the cost is higher, switching regulators are normally more efficient than linear regulators. Efficiency is the overriding factor for

most of the system design. For instance, modern signal processing system and wireless communication systems will use different supply voltages to minimize power loss and extend battery life. For power electronic loads, DC-DC converter also can be used as intermediate stage before connect to the load supplying DC-DC converter, which can improve power factor.

1.3 APPLICATION OF DC-DC BOOST CONVERTER

DC-DC boost converter has an immense range of application. It allows target applications working with a power supply has lower level than the operating voltage. Normally, it can also be used as a regulator for noisy power source to reduce the voltage ripple. For low power applications, especially battery powered devices, boost converter can reduce the number of battery being used since the required input voltage level is reduced. For instance, a LED light can be driven by single 1.5V alkaline cell battery after connecting boost converter, which let the size of battery times smaller. Nowadays, portable device has great demand of reducing size, which let boost converter being an ideal solution. Meanwhile, regulated output also protect device being damage if applicant is sensitive to noise, such as consumer electronic devices. It is expected that modern portable wireless communication and signal processing systems will use variable supply voltages to minimize power consumption and extend battery life [1.5]. But like the RF antenna, higher output may be needed to improve the transmission performance. Boost converter become a convenient solution in this case. Output voltages of dc–dc converters range from a volt for special VLSI circuits to tens of kilo- volts in X-ray lamps. If original signal has very low amplitude such as bioelectric signal, high transform ratio can be used therefore the output level will become more suitable for further processing.
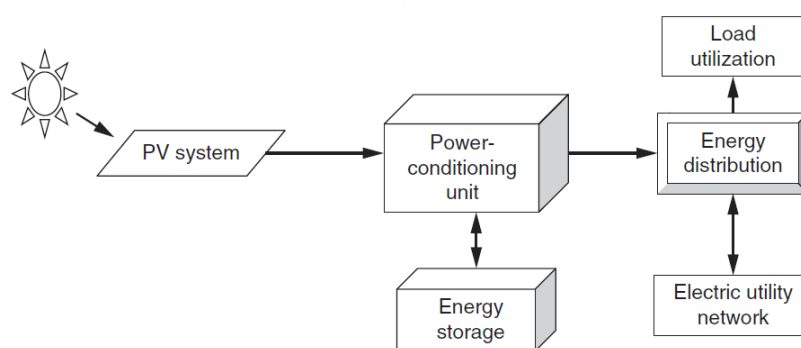

Figure 1.3.1 Major photovoltaic system component [1.5]

Another typical application field of boost converter is renewable energy system. Energy being harvested can store by battery or directly connect to the power grid. In solar energy system, boost converter allows the number of photovoltaic (PV) panels used as input be reduced. Concurrently, output quality can be ensured. If battery is used as the energy storage, their lifetime can be expanded. As an additional power inject into power grid, power quality of grid will not be deteriorated. Above figure shows a grid-connected photovoltaic system which is composed of PV arrays connected to the grid through a power conditioning unit and are designed to operate in parallel with the electric utility grid. The power conditioning unit may include the MPPT (Maximal Power Point Tracking), the inverter, boost converter as well as the control system needed for efficient system performance.

After the input become higher than grid voltage level, boost converter usually used to regulate input. For AC input, it can be used to correct power factor which is called power factor correction. It shapes the input current of power supply to maximize the real power available from the mains [1.6]. Current scheme for AC to DC power conversion typically involve two stages. It is composed of an input boost power factor corrector which convert the input and pre-regulate the input line to 190V (for 110V/AC power line). The bus then provides the input voltage for a conventional DC-DC converter which can be appropriate technology.
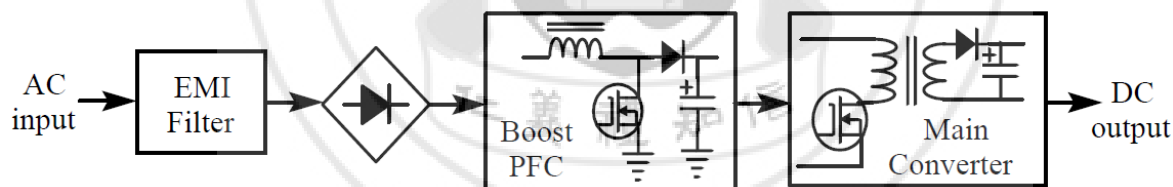
Figure 1.3.2 Conventional PFC conversion stage [1.6]

1.4 OVERVIEW OF DC-DC CONVERTER

In fact, DC-DC converter shows a bright future in both research and merchant field. By summarized paper published in IEEE on the transaction of power electronics to find out the trends of research interest of power electronics in recent two years, which shows that power converter was the most popular topic until now. Among different conversion types, DC-DC converter shows its higher preference to researchers. For most of the electronic devices they should have one or more regulators for obtain a stable voltage which is higher or lower than input. For some sensitive equipment like analog circuit, DC-DC regulator can also regulate the voltage ripple in certain range

to protect the components [1.7]. Depends on target appliance, different topologies can be used to achieved a better performance. For instance, linear regulator usually be used as power supply of data converter since it provides very low voltage ripple; Switching regulator is widely used in digital signal processor since they provide high efficiency. Above discussion already shows the research in this area already popular for years. Especially when we consider the fast-growing consumer electronics market, more products were put into the market, while efficiency is one of the greatest demand for them. There will be a wider range of use for DC-DC converter in the future, and it is certainly an area worthy to work on.

1.5 TARGET APPLICATION

Table 1.5.1 shows six possible applications for the proposed KY converter. The transfer characteristic of KY converter decided the output voltage is between one and two times of input voltage. Detailed explained will be shown in following chapter. Since low power applications usually requires boost converter perform high transform ratio to reduce the size of input source, therefore, target will focus on relative higher power applications.

	Input Voltage	Output Voltage	Frequency	Rating Power
Lighting Device	9V	12V	20MHz	60W
Communication Equipment	12V	16V	5MHz	15W
Uninterruptible Power Supply	36V	48V	1MHz	1KW
Power Factor Correction	230V	400V	200KHz	1.5KW
PV Panel Output [1.8]	500v	750V	19KHz	10KW
DC Microgrid Application [1.9]	200V	500V	15KHz	1KW

Table 1.5.1 Possible applications for KY converter

In this project, proposed KY converter will be assumed to use as a link between PV panel and conventional power grid. From literature review, renewable energy seems was a popular topic in

past years and this trend should maintain in the future. Among various renewable energy fields, photovoltaic for solar energy is one of the most mentioned field which is not difficult to implement. After consider the component rating and safety for experiment, output side of KY converter is assumed to connect and directly inject power. In this case, output voltage should at least equal to root means square value of power grid voltage, which is 190.53V for a 110V/AC three phase power grid. Moreover, small output voltage ripple should be considered, which means setting value should be slightly higher grid level. Hence, the proposed output voltage level is assumed to be 200V. Basic structure for this solar energy system is shown in figure 1.5.1. From data sheet of a conventional PV panel [1.10], output voltage for maximal power point is stated as 32.4V. Therefore, PV string consist of four series connected panels can output power at 129.6V. Proposed input voltage level will be assumed as 130V. After the power being regulated by KY converter, it will pass through a DC/AC converter before inject into grid or other domestic AC loads. Specification for KY converter in proposed application is summarized in table 1.5.2.
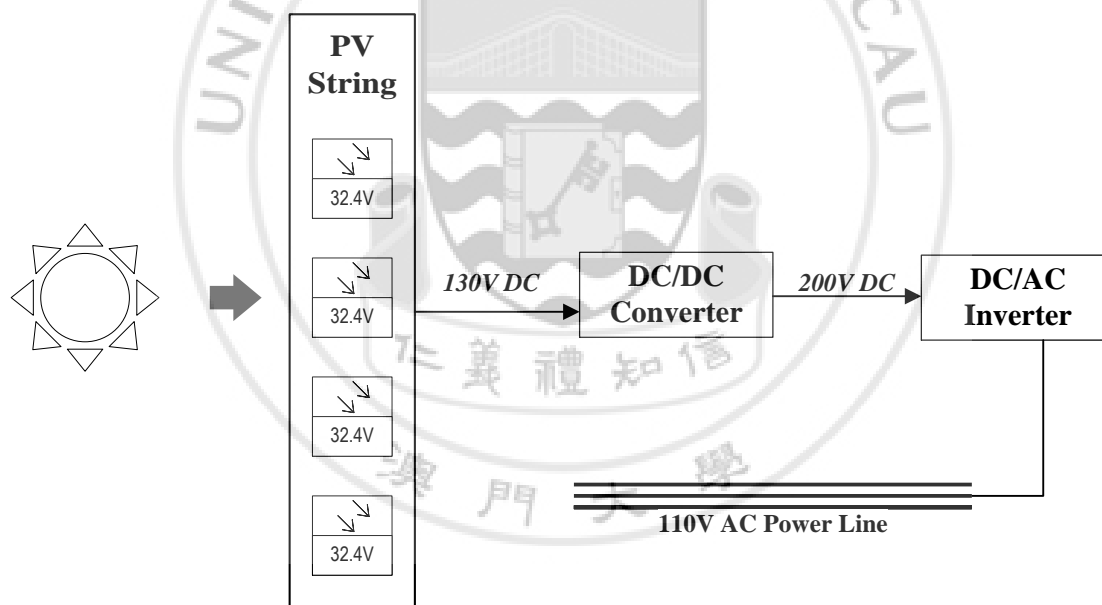

Figure 1.5.1 Solar energy system

Input Voltage	Output Voltage	Switching Frequency	Power Rating
130V	200V	15KHz	1.6KW

Table 1.5.2 Specification for proposed application

CHAPTER 2: ANALYSIS OF KY CONVERTER

2.1 OVERVIEW OF KY CONVERTER

KY converter is a dc-dc converter for step up voltage, proposed by Hwu, K.I. and Yau, Y.T in 2009. It is composed by a buck converter and a switched-capacitor charge pump converter. Compare to conventional non-isolated boost converter, it offers fast transient response, non-pulsating output current, low output voltage ripple and no RHPZ during continuous conduction mode [2.1]. Figure 2.1 shows the circuit diagram of KY converter. Switching of power transistor is controlled by a duty cycle D on PWM signal.
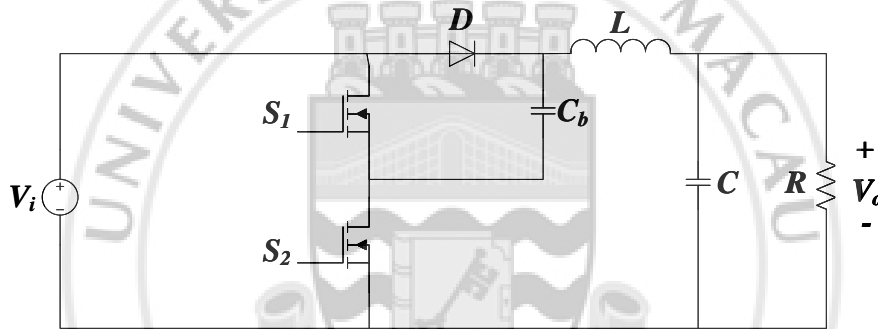

Figure 2.1 The schematic of KY Converter

2.2 OPERATION PRINCIPLE

Overall, conversion is based on power switch periodically switching to let power transfer from input to output. In KY converter as shown in figure 2.1, two switches S_1 and S_2 will conduct alternatively. Turn on/off time for each of them is controlled by duty cycle D. As the media, inductor will absorb and release energy in different period to let it pass from input to output. Depends on the continuity of inductor current, KY converter's operation can be divided into two modes: Continuous Conduction Mode (CCM) and Discontinuous Conduction Mode (DCM).

2.2.1 CCM ANALYSIS OF KY CONVERTER

Figure 2.2.1 shows waveform of inductor voltage and current during CCM. One switching cycle T_s will be divided into two parts: When device is running between time interval $0 < t < DT_s$, S_1 is turned on and S_2 is turned off during this period. Inductor will absorb energy during this period and the inductor current i will increase. If time is turn into interval $DT_s < t < T_s$, S_1 will turn off and S_2 will turn on. Inductor will release energy and its current will decrease.
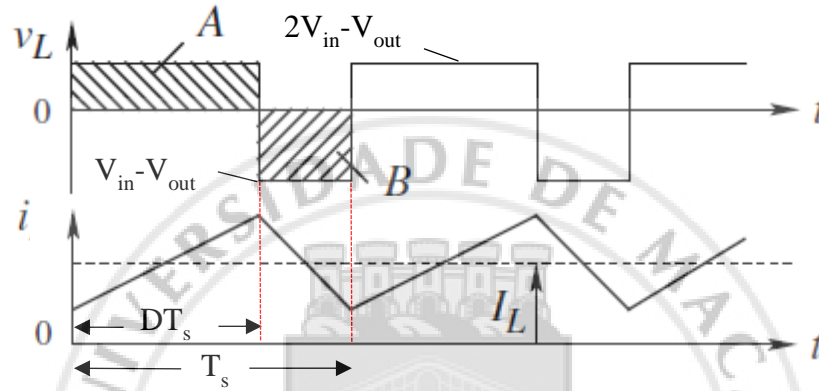

Figure 2.2.1 Inductor current and voltage [2.2]

During state 1 ($0 < t < DT_s$), power will flow as shown in figure 2.2.2. Diode D_b will not conduct, the voltage across flying capacitor V_{cb} will be discharged to Vin within very short period. Base on Kirchhoff's Current Law and Kirchhoff's Voltage Law, the sum of input voltage V_i, V_{cb} and output voltage across output capacitor C will be equal to inductor voltage V_L. Output capacitor current i_C will equals to inductor current minus the current pass through output resistor i_R. Consequently, following Eq. (2.1) can be deduced.
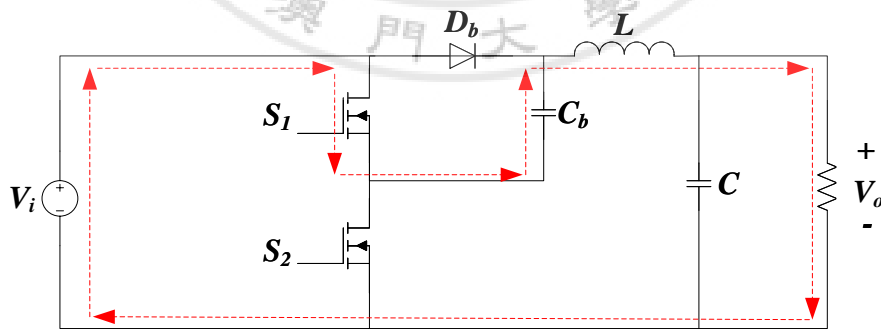

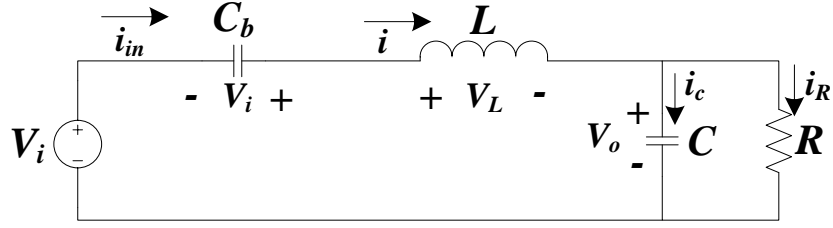Figure 2.2.2 Power flow when S_1 is turned on and S_2 is turned off (state 1)

14

Figure 2.2.3 Equivalent circuit for KY converter in state 1

$$\begin{cases} V_L = V_i + V_{cb} - V_o = 2V_i - V_o = L\dfrac{\partial i}{\partial t} \;\; (V_{cb} = V_i) \\[2mm] i_C = C\dfrac{\partial v_o}{\partial t} = i - \dfrac{V_o}{R} \\[2mm] i_{in} = i \end{cases} \tag{2.1}$$

During state 2 ($DT_s < t < T_s$), S_1 will turn off and diode will conduct. After C_b being discharged to input voltage V_i, energy transfer capacitor will form a loop with inductor and output capacitor, which let the inductor voltage equals to the difference between input and output voltage. Input current will flow through L and C_b in different way. This state can be described by (2.2).
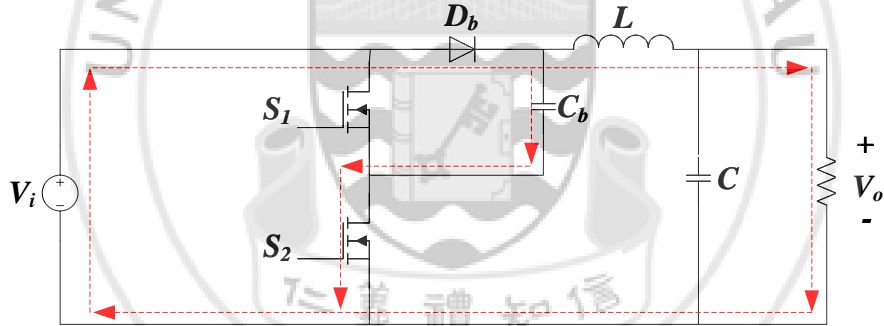

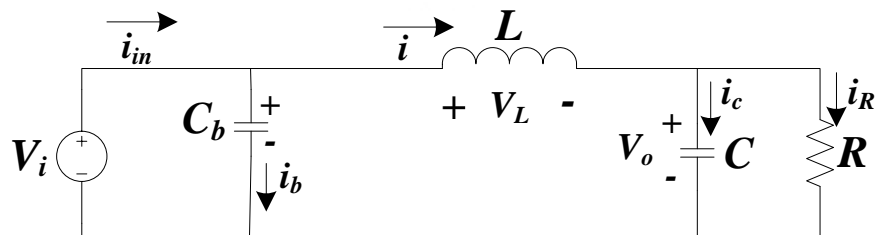Figure 2.2.4 Power flow when S_1 is turned off and S_2 is turned off (state 2)

Figure 2.2.5 Equivalent circuit for KY converter in state 2

15

$$\begin{cases} V_L = L\dfrac{\partial i}{\partial t} = V_i - V_o \\[2mm] i_C = C\dfrac{\partial v_o}{\partial t} = i - \dfrac{V_o}{R} \\[2mm] i_{in} = i + i_b \end{cases} \tag{2.2}$$

After obtain equations for both states, (2.3) can be used to average the differential terms. Therefore, the average equation can be obtained as (2.4).

$$\bar{x} = \frac{1}{T_s}\int_{0}^{T_s} x\, d\tau \tag{2.3}$$

$$\begin{cases} L\dfrac{\partial i}{\partial t} = (1+d)V_i - V_o \\[2mm] C\dfrac{\partial v_o}{\partial t} = i - \dfrac{V_o}{R} \\[2mm] i_{in} = i + i_b \end{cases} \tag{2.4}$$

Therefore, input and output relationship in steady state can be obtained.

$$\begin{cases} 0 = (1+D)V_i - V_o \\[2mm] 0 = i - \dfrac{V_o}{R} \\[2mm] i_{in} = (1+D)i \end{cases} \tag{2.5}$$

$$\frac{V_o}{V_i} = \frac{i_{in}}{i} = 1 + D \tag{2.6}$$

In further, by substitute original component value to dc quiescent value $|x|$ plus the superimposed ac variation $\hat{x}$ as shown in (2.7) into (2.4), (2.8) can be obtained. Finally, small signal equation can be derived by neglected second order as terms.

$$\begin{cases} V_i = V_i + \widehat{V}_i \\ d = D + \hat{d} \\ i = I + \hat{i} \\ V_o = V_o + \widehat{V}_o \\ i_{in} = i_{in} + \widehat{i_{in}} \end{cases} \tag{2.7}$$

$$\begin{cases} L\dfrac{\partial I + \hat{i}}{\partial t} = (1 + D + \hat{d})(V_i + \widehat{V_i}) - V_o + \widehat{V}_o \\[2mm] C\dfrac{\partial V_o + \widehat{V}_o}{\partial t} = (I + \hat{i}) - \dfrac{V_o + \widehat{V}_o}{R} \\[2mm] i_{in} + \widehat{i_{in}} = (1 + D + \hat{d})(I + \hat{i}) \end{cases} \tag{2.8}$$

$$\begin{cases} L\dfrac{\partial \hat{\imath}}{\partial t} = (1+D)\widehat{V_\imath} + \hat{d}V_i - \widehat{V_o} \\[2mm] C\dfrac{\partial \widehat{V_o}}{\partial t} = \hat{\imath} - \dfrac{\widehat{V_o}}{R} \\[2mm] \widehat{\imath_{\imath n}} = (1+D)\hat{\imath} + I\hat{d} \end{cases} \tag{2.9}$$

From the small signal as shown in figure 2.2.6, open loop transfer function can be obtained.

$$T_{CCM} = \frac{V_i}{LCs^2 + \dfrac{L\sqrt{LC}s}{R} + 1} \tag{2.10}$$
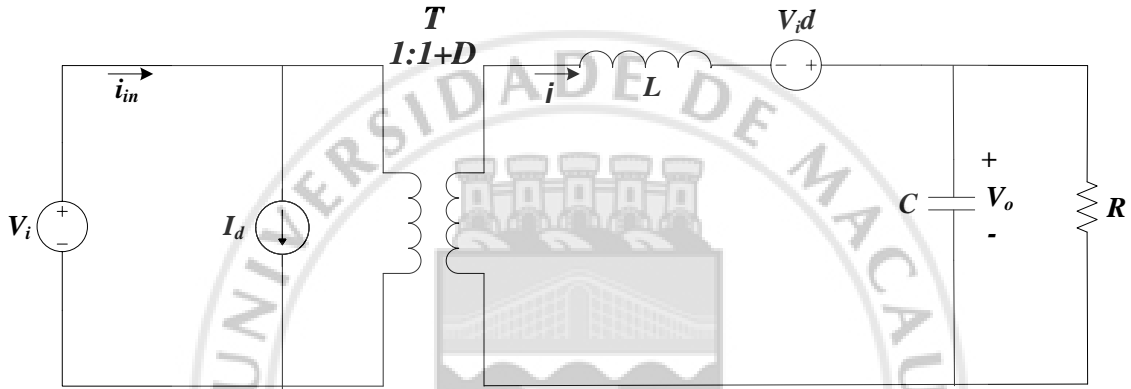
Figure 2.2.6 Small signal model for KY converter in CCM

Above deduction results are based on the neglect the raising time of voltage V_{cb} across C_b, but its variation should be taken account into the calculation for improve accuracy. Since energy is flowing between energy transfer capacitor and inductor, charges variation of them should be equal base on charge conservation. Assume V_{cb} decrease in slope equals to $-i/C_b$, (2.11) shows the expression for V_{cb} [2.3]. Switching frequency is represented by f.

$$V_{cb} = V_i - \frac{i}{2fC_b}D^2 \tag{2.11}$$
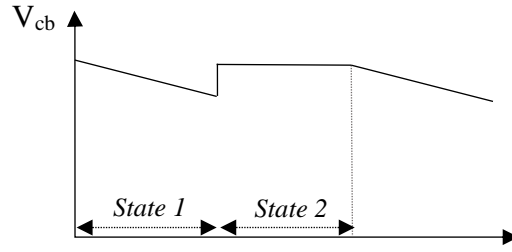
Figure 2.2.7 Flying capacitor variation phenomena

Finally, transfer function of KY converter in CCM can be obtained

$$T_{CCM}(s) = \frac{\dfrac{V_i}{LC} - \dfrac{3D^2 I}{2LCfC_b}}{s^2 + \left(\dfrac{D^3}{2fLC_b} + \dfrac{1}{RC}\right)s + \dfrac{D^3}{2RfLC_bC} + \dfrac{1}{LC}} \qquad (2.12)$$

2.2.2 BOUNDARY OF CCM AND DCM ON KY CONVERTER

If KY converter is working on the boundary between CCM and DCM, inductor will be totally demagnetized exactly the end of each cycle. Figure 2.2.8 shows the inductor current waveform when converter is working on boundary.

Figure 2.2.8 Inductor waveform of KY converter in boundary of CCM and DCM

Assume it change linearly as equation (2.13), following equations can be obtained.

$$i = \frac{V_L}{L} \qquad (2.13)$$

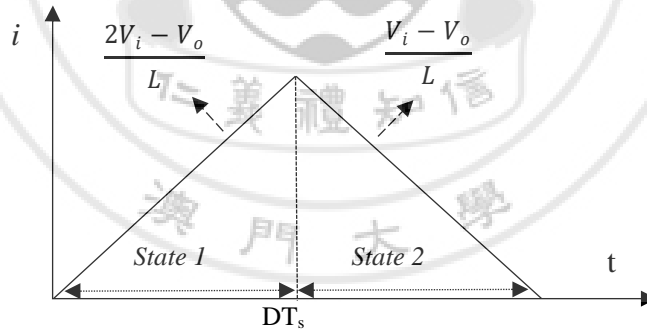$$\Delta i = i(DT_s) = \frac{(2V_i - V_o)DT_s}{L} = \frac{(2V_i - V_o)D}{fL} \tag{2.14}$$

$$L = \frac{(2V_i - V_o)D}{2f i_{OB}} \tag{2.15}$$

For a fixed load resistance and output voltage, inductance can be expressed as (2.15), which shows the increment of frequency can reduce the size of inductor. Average dc output load current at the boundary can be determined. Resistance for pure resistive load can be expressed as (2.17).

$$i_{OB} = \frac{\Delta i}{2} = \frac{(2V_i - V_o)D}{2fL} = \frac{(1-D)D}{2fL} \tag{2.16}$$

$$R_{LB} = \frac{V_o}{i_{OB}} = \frac{2Lf(1+D)}{(1-D)D} \tag{2.17}$$

For $K = 2Lf/R_L$, normalized load current and resistance waveform at the CCM/DCM boundary as a function of duty cycle D for KY converter can be plotted out.
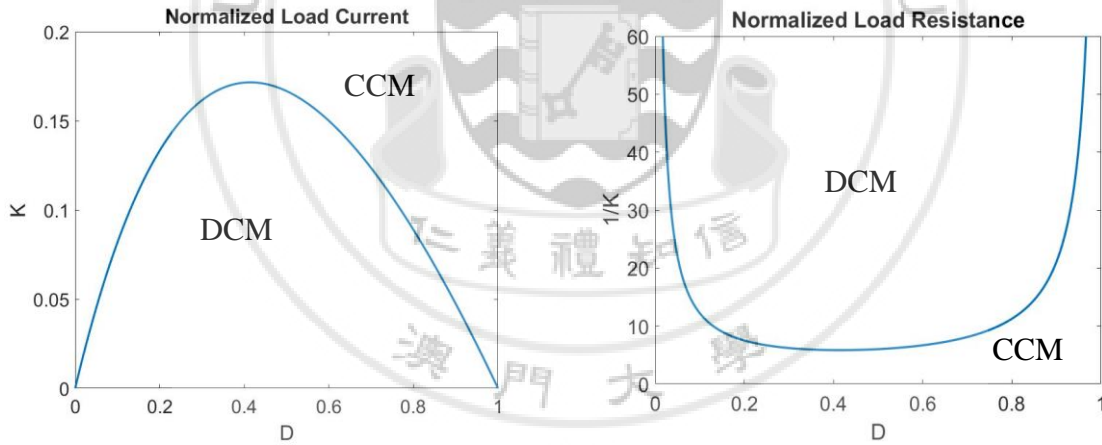
Figure 2.2.9 CCM/DCM boundary for normalized load current and resistance

2.2.3 DCM ANALYSIS OF KY CONVERTER

Figure 2.2.10 shows the inductor waveform when converter is working in DCM. Compare to CCM, inductor current still increase to its maximal level when $0 < t < DT_s$. However, it will drop to zero before $t = T_s$. Original state 2 in CCM will be further divided into state 2-a and state 2-b, which is shown as the duration D_1 and D_2 in the figure. Since no current will flow through the inductor

19

during state 2-b, the power will flow between output capacitor and load resistor as shown in figure 2.2.11. Based on ampere-second balance, transfer function during steady state can be obtained from (2.18).
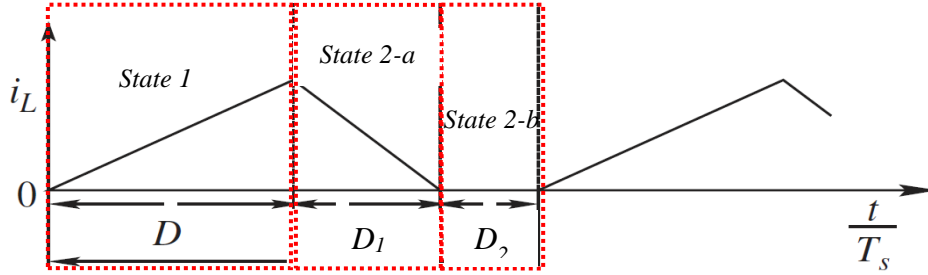
Figure 2.2.10 Inductor current waveform during DCM
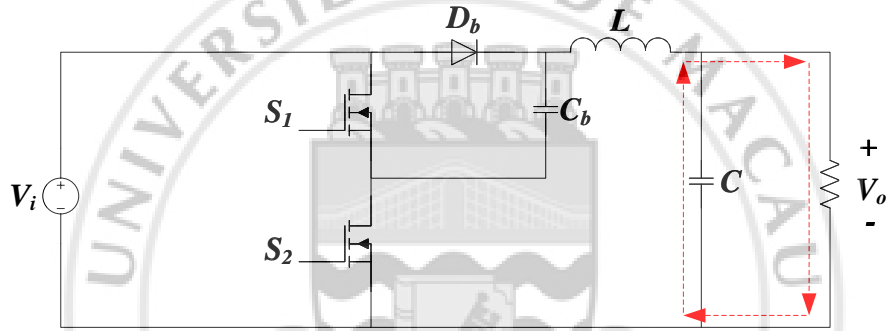
Figure 2.2.11 Power flow of KY converter in state 2-b

$$2(V_i - V_o)DT = (V_i - V_o)D_1T \qquad (2.18)$$

$$T_{DCM} = \frac{V_o}{V_i} = \frac{2D + D_1}{D + D_1} \qquad (2.19)$$

Therefore, dc load current I_{load} can be expressed as

$$I_{Load} = \frac{1}{T}\int_0^T iTdt = \frac{(D + D_1)\Delta i}{2} = \frac{2(V_i - V_o)D(D + D_1)}{2fL} \qquad (2.20)$$

By finding D_1 in (2.19) and substitute into (2.20), transfer function become

$$T_{DCM} = \frac{V_o}{V_i} = \frac{\left(1 - \frac{D^2}{k}\right) + \sqrt{1 + \frac{D^4}{k^2} + \frac{6D^2}{k}}}{2}, \ k = \frac{2Lf}{R} \qquad (2.20)$$

Flying capacitor V_{cb} variation need to be considered for deduce small signal model. R_{eq} is equivalent resistance for represent V_{cb} variation. Since the inductor average inductor current in one cycle is changed to (2.22), V_{cb} will be variate as (2.23).

$$\bar{\imath} = \frac{\Delta i}{2}(D + D_1) \tag{2.21}$$

$$\Delta Vc_b = \frac{D\bar{I}}{fC_b(D + D_1)} \tag{2.23}$$

Therefore, R_{eq} can be obtained as

$$R_{eq} = \frac{\Delta Vc_b}{\bar{\imath}} = \frac{D\bar{I}}{fC_b(D + D_1)} \tag{2.24}$$

After that, transfer function for DCM will be modified after consider V_{cb} variation.

$$T_{DCM} = \frac{-(kD^2b - k^2b - 4D^5) + \sqrt{-4(k^2b + D^5)(4D^5 - 2kD^2b) + (kD^2b - k^2b - 4D^5)^2}}{2} \tag{2.25}$$

Where b = 2fCR.

By using same deduction method for buck converter [2.4], a small signal model of KY converter for DCM can be deduced as figure 2.2.12. r_L and r_C represent the equivalent resistance for inductor and output capacitor.
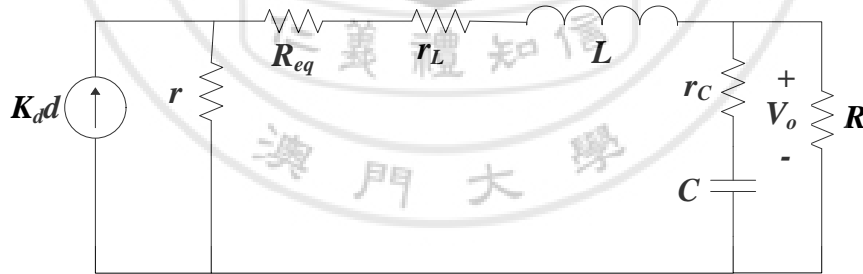

Figure 2.2.12 Small signal model for KY converter of DCM

k_d and r in figure 2.2.12 can be expressed as

$$K_d = \frac{2V_o}{R}\sqrt{\frac{2 - T_{DCM}}{kT_{DCM}(T_{DCM} - 1)}} \tag{2.26}$$

$$r = \frac{R(2 - T_{DCM})(1 - T_{DCM})}{T_{DCM}} \tag{2.27}$$

21

In further, small signal transfer function of KY converter in DCM can be found:

$$G_{vdcm}(s) = H \frac{1 + \frac{s}{z}}{1 + p_1 s + p_2 s^2} \tag{2.28}$$

Where

$$H = K_d \frac{rR}{r + R + R_{eq} + r_L} \tag{2.29}$$

$$z = \frac{1}{r_c C_b} \tag{2.30}$$

$$p_1 = \frac{L + C_b((R + r_c)(r + r_L + R_{eq}) + Rr_c)}{r + R + R_{eq} + r_L} \tag{2.31}$$

$$p_2 = LC_b \frac{R + r_c}{R + r + R_{eq} + r_L} \tag{2.32}$$

2.3 SIMULATION VERIFICATION OF KY CONVERTER THEORY

To verify the correctness of above analysis, a KY converter is built in PSCAD/EMTDC for simulation. Parameters being used during simulation is shown in table 2.3.1. Diode forward voltage drop is set as 0.6V. Schematic for simulation is shown in figure 2.3.1.

V_{in} (V)	Duty Ratio	f_s (kHz)	L (µH)
130	0.2 – 0.8	15	120
C_b (mF)	C_o (mF)	R_{Load} (Ω)	
1	1	25 - 100	

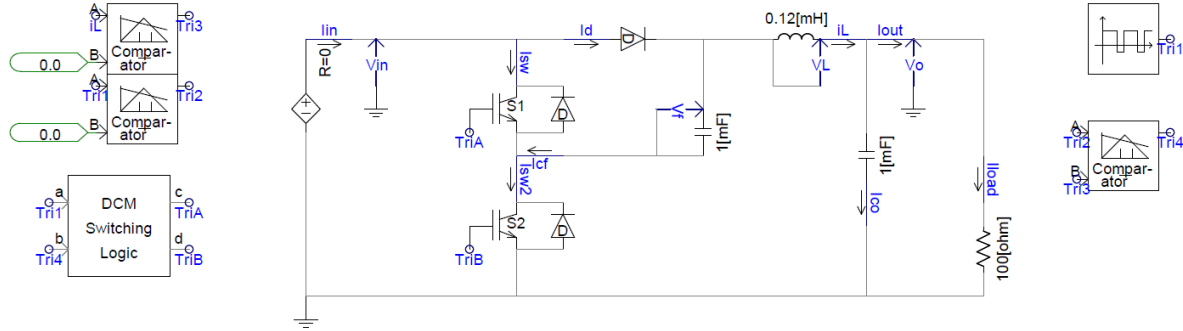Table 2.3.1 Simulation parameters for KY converter

Figure 2.3.1 PSCAD simulation schematic of KY converter

As mentioned in previous section, difference of circuit behavior in CCM can be reflected on the inductor current. Its waveform in two conduction modes in simulation is shown in figure 2.3.2. During the simulation, various input voltage level and duty ratio had been applied to find out the error between simulation result and theoretical value base on (2.12)
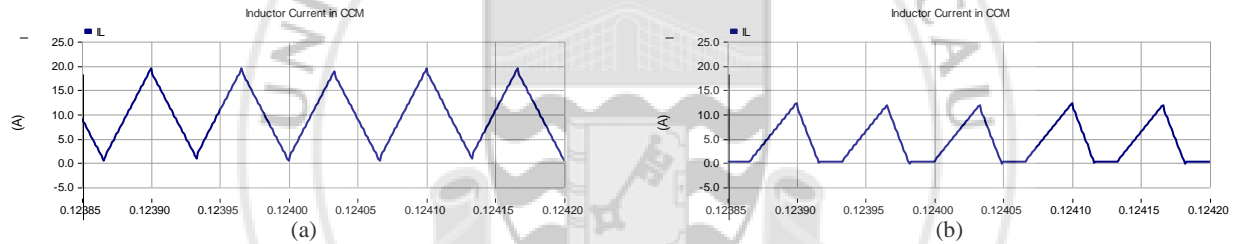

Figure 2.3.2 Inductor current waveform in (a) CCM and (b) DCM during simulation

V_{in} (V)	D = 0.2	D = 0.4	D = 0.6	D = 0.8
110	0.11%	0.14%	0.09%	0.25%
130	0.11%	0.17%	0.07%	0.27%
150	0.11%	0.15%	0.1%	0.27%

Table 2.3.2 Error between theoretical and simulation output voltage value in CCM

As the result shown in table 2.3.2, gain for KY converter in open loop perform no more than 0.86% variation from calculation result based on theory. Furthermore, figure 2.3.3 shows the verification of DCM result on the specifically. For gain of KY converter in DCM, change in inductance, load resistance and switching frequency will also have observable effect on converter's behavior. Figure 2.3.3 shows the plots of DC transfer function M_{VDC} versus the normalized load resistance $R_{Load}/2fL$ and normalized load current $I_{load}/(V_{out}/2fL)$. The red line represents the boundary, while black line shows the theoretical gain of KY converter in different duty ratio. The cross point "x"

23

indicates the simulation result. Overall, this part of simulation results show that the behavior of KY converter in both CCM and DCM is follow the expected trends.
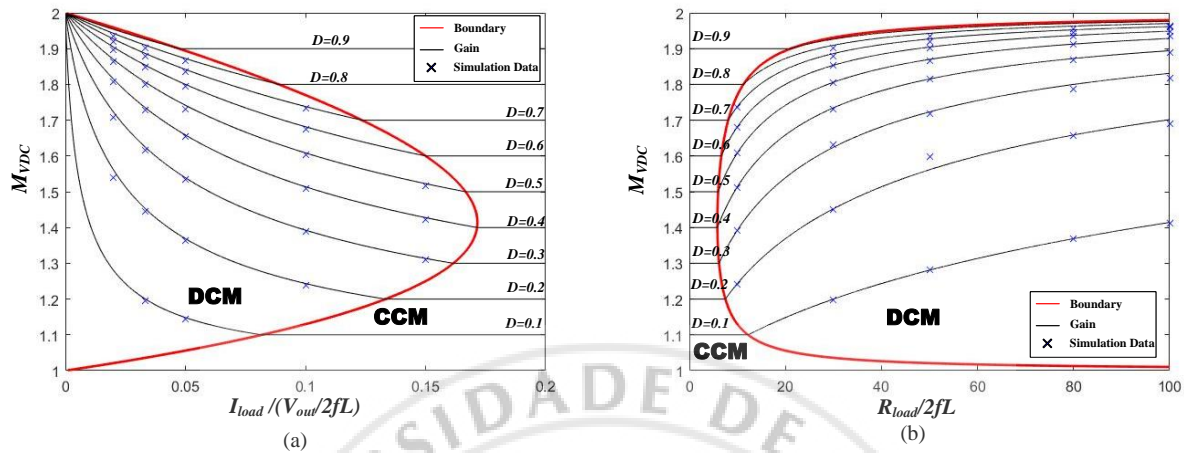

Figure 2.3.3 KY converter gain versus the normalized (a) Load resistance and (b) Load current

CHAPTER 3: CLOSE LOOP CONTROL OF KY CONVERTER

3.1 OVERVIEW OF CLOSE LOOP CONTROL

Close-loop control for dc-dc converter is necessary for improve overall system performance. For most of the electrical system, input and load condition always changing. Meanwhile, components value will change with temperature, pressure and time. Actual output level usually various from the expected in open loop system. In close-loop system, output will be measured to adjust the system which aims to improve the stability and accuracy of overall system. Figure 3.1.1 shows a typical block diagram of close-loop control topology.
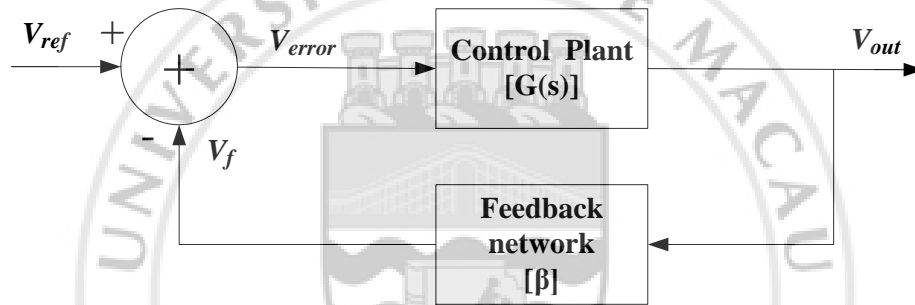
Figure 3.1.1 Typical close-loop control diagram

By set up an expected value, error of output can be sensed as an error signal and passed to control plant for further processing. Control plant in above figure represents the original power stage, pulse width modulator and related control logics, meanwhile the lower block represents the feedback network. Normally, output will be measured as a negative feedback which sum up with a reference value. Depends on system characteristic, various control methods can be used, but in general, it processes the signal from feedback for adjust the output as reference. Overall, application of close loop control in KY converter can be described as extend of above diagram as shown below. In following sections in this chapter, details of each part of close-loop approach of proposed KY converter will be discussed.
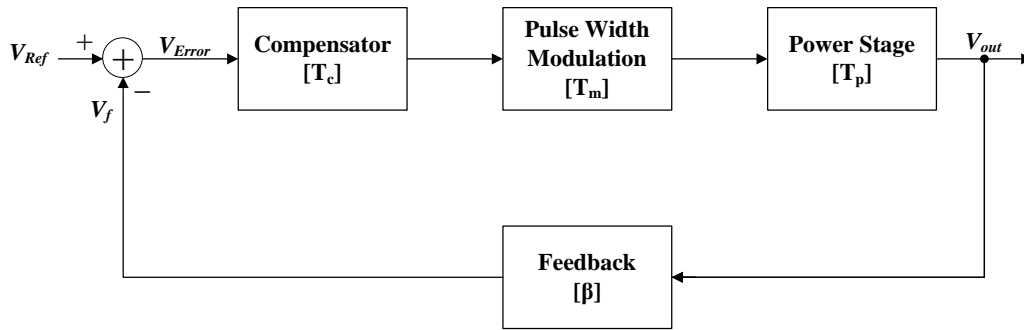
Figure 3.1.2 Close loop control block diagram of KY converter

3.2 VOLTAGE AND CURRENT MODE CONTROL

Voltage mode control and current mode control are the most common-used control method for PWM dc-dc converter. In figure 3.2.1, schematic for voltage and current mode control for boost converter is shown as reference. They only distinguish by the signal to be compare with error signal in pulse width modulator.

(a)   (b)

Figure 3.2.1 Schematic of (a) Voltage mode control and (b) Current mode control [3.1]

After the converter output is sensed and subtracted by an external reference voltage in an error amplifier, in will be passed to a pulse width modulator, which is used for generated the control

signal for power switches. In voltage mode control, error is compare with a saw-tooth waveform. Switching frequency can be variate by change the frequency of saw-tooth signal, which is provided by external sources. While in current mode control, it requires an additional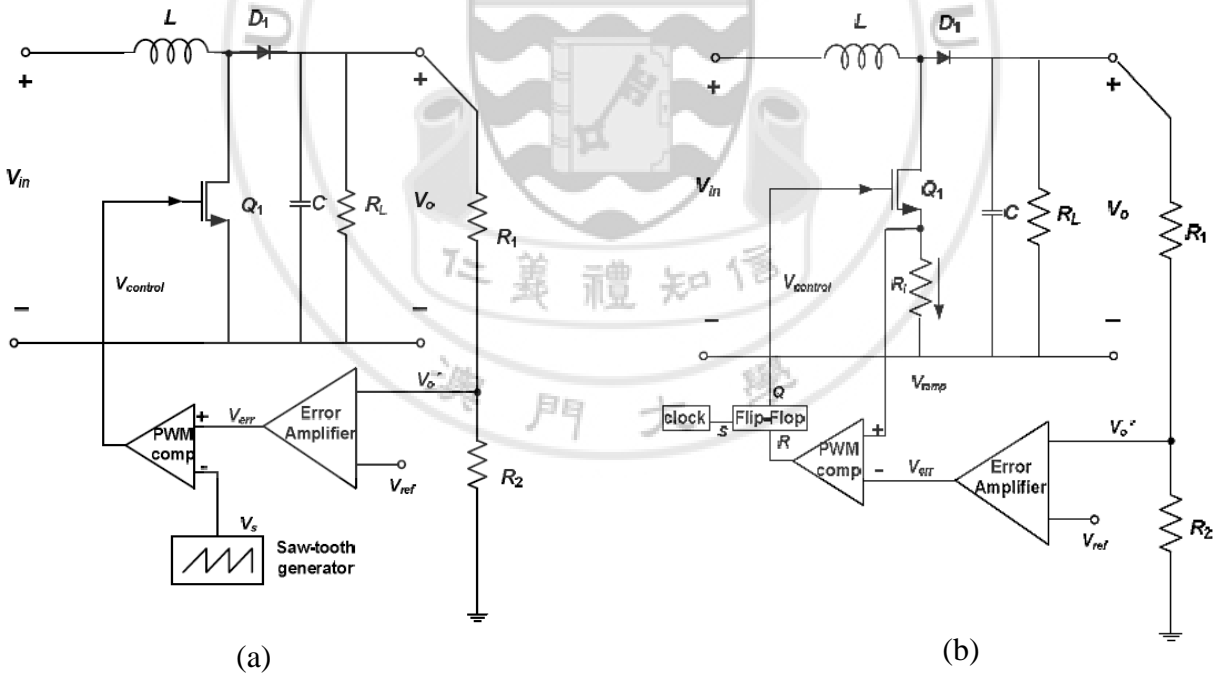 inner signal for feedback loop of certain parameters, which is inductor current in figure 3.2.1. When the inductor current reaches the peak, it is naturally equals to the peak switch current. Then, the latter can be used in inner loop which simplified the current sensor. By provided an external signal to Flip-Flop, current mode control can maintain in constant frequency. In comparison, voltage mode control is easier to implement since it requires less components. Besides, current mode control will occur sub-harmonic oscillation if the duty cycle is too large. More importantly, simpler principle for voltage mode control lets further design has more flexibility. Therefore, voltage mode control was chosen in this project.

3.3 CLOSE LOOP CONTROL CIRCUIT IN KY CONVERTER

3.3.1 FEEDBACK NETWORK

Output voltage will be sensed by a feedback network to transform the signal to appropriate level. Typically, there are three types of feedback approaches being used for perform as a voltage divider, or along with phase lead and lag function. Their structure and equivalent transfer functions can be found in table 3.1.

Type	(a)	(b)	(c)
Circuit Diagram	*Vout* — R_A — V_f — R_B	*Vout* — R_A — V_f — R_B — C_1	*Vout* — R_A ‖ C_1 — V_f — R_B
Transfer Function (β)	$\dfrac{R_B}{R_A + R_B}$	$\dfrac{R_B}{R_A + R_B} \dfrac{1}{\left(1 + \frac{sC_1 R_A R_B}{R_A + R_B}\right)}$	$\dfrac{R_B}{R_A + R_B} \dfrac{1 + sC_1 R_A}{\left(1 + \frac{sC_1 R_A R_B}{R_A + R_B}\right)}$

Table 3.1 Feedback network schematics and their transfer function

Type (a) feedback is a voltage divider, which can generate a feedback voltage V_f in different voltage level but has no effect on frequency. Base on this network, add a capacitor in parallel with one of the resistor can create a pole or both zero and pole, which allows the network achieves lead or lag function by effecting the frequency. In this project, a compensator will be further connected with this feedback network to adjust the phase margin. For here, feedback network doesn't require the ability of adjust the signal in frequency domain. It will overlap with the function of compensator and create unnecessary waste. Type (a) network is preferred here since it involves least components and design consideration.

3.3.2 COMPENSATOR

In conventional closed-loop control power converters, different types of compensators are widely used for provide enough phase margin, which aims to improve overall system stability. By connect various number of resistors and capacitors with an op-amp, phase margin of the signal can be changed in the range of 0 to 180 degrees. In table 3.2, schematics of three types of compensator are shown along with their poles and zeros location.
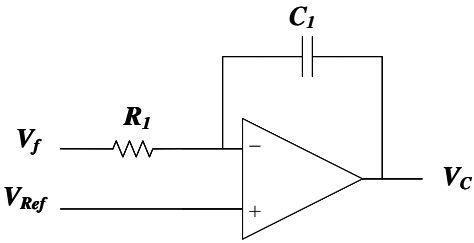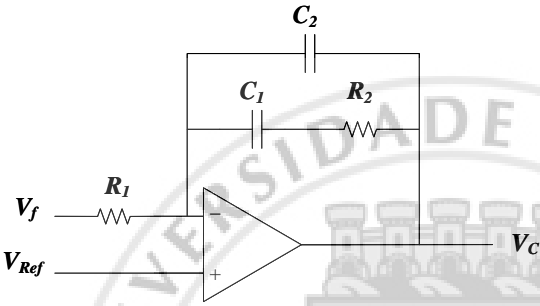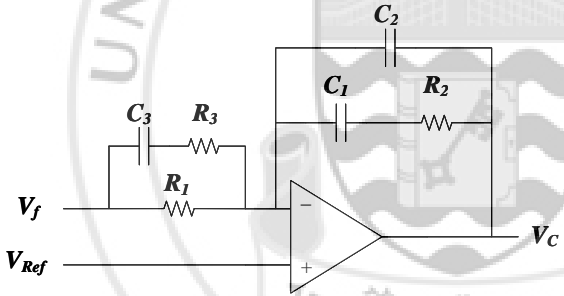
Type	Circuit Diagram	Zeros	Poles
I	C_1 R_1 V_f V_{Ref} V_C	None	$P = \dfrac{1}{2\pi R_1 C_1}$
II	C_2 C_1 R_2 R_1 V_f V_{Ref} V_C	$Z = \dfrac{1}{2\pi R_2 C_1}$	$P_1 = 0$ $P_2 = \dfrac{1}{2\pi R_2 C_2}$
III	C_2 C_1 R_2 C_3 R_3 R_1 V_f V_{Ref} V_C	$Z_1 = \dfrac{1}{2\pi R_2 C_1}$ $Z_2 = \dfrac{1}{2\pi C_3 (R_1 + R_3)}$	$P_1 = 0$ $P_2 = \dfrac{1}{2\pi R_1 C_3}$ $P_3 = \dfrac{C_1 + C_2}{2\pi R_2 C_1 C_2}$

Table 3.2 Schematics of compensators and their pole-zero location

Type I compensator indeed is an integrator which can affect the system by add pole and cause maximal 90-degree phase shift. Since the goal of uses of compensator is to improve phase margin, this type of compensator will not be considered here. By adding a series RC into type I compensator, one more pole and zero can be provided, which becomes a type II compensator. The extra pole-zero can provide maximal 90-degree boost in margin theoretically. Equivalently, type III compensator has an extra RC in series connected with the circuit than type II, which let it contain two pole-zero pairs and one pole at the origin as shown in table 3.2.
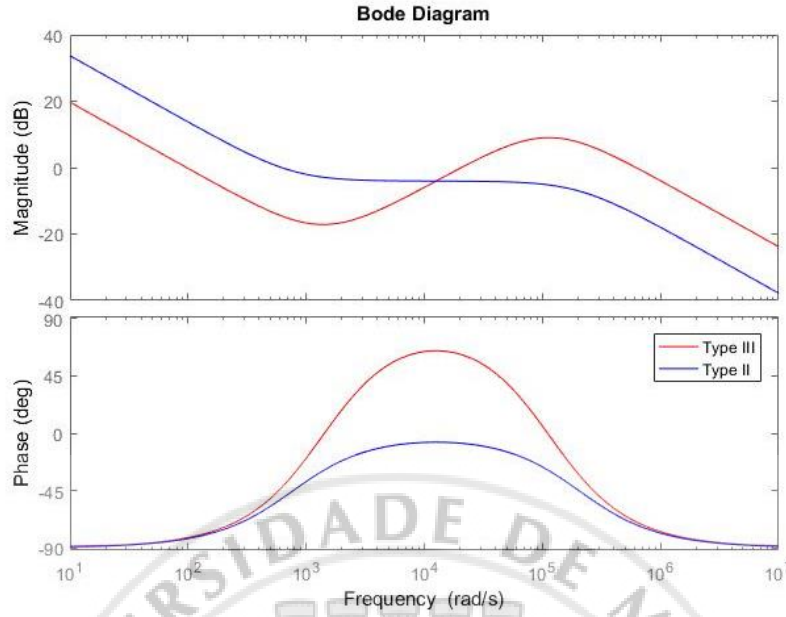
Figure 3.3.1 Bode plot of type II and type III compensator

Figure 3.3.1 illustrates a typical bode plot of typical type II and type III compensator. Type III compensator has double the ability in boost up phase margin in compare to type II, which increase the flexibility and possibility in system design. If the phase lag of power converter can approach 180 degree, the maximal phase from a type II compensator at any frequency is at most zero degree. Hence, type III compensator will be used in proposed design to provide enough phase margin to keep the stability of system. From poles and zeros information as shown in table 3.2, its transfer function can be represented as equation (3.1).

$$T_c(s) = \frac{(s + Z_1)(s + Z_2)}{(s+P_1)(s+P_2)(s+P_3)} = \frac{R_1 + R_3}{C_2 R_1 R_3} \times \frac{\left(s + \frac{1}{R_2 C_1}\right)\left[\left(s + \frac{1}{C_3(R_1 + R_3)}\right)\right]}{s\left(s + \frac{C_1 + C_2}{R_2 C_1 C_2}\right)\left(s + \frac{1}{C_3 R_1}\right)} \tag{3.1}$$

3.3.3 PULSE WIDTH MODULATOR

Pulse-Width-Modulation (PWM) is widely used in DC-DC converter circuit, in order to provide variable gate signal to power switches to change the output voltage level. Figure 3.2.3 illustrates the generation of PWM signal in this system.

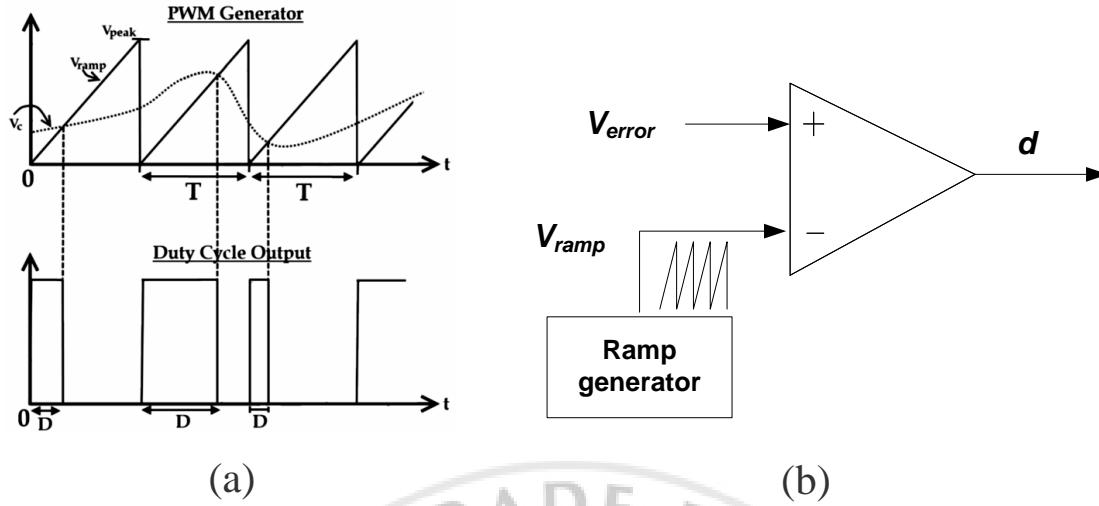(a)   (b)

Figure 3.3.3 (a) Waveform of PWM generation and (b) its circuit

After feedback signal from output being compensated, the control signal V_c will be used to compare to a saw tooth signal, which is given by a ramp generator. The comparison generates a pulse output in different width. Once the control signal become higher (i.e. error become bigger, output become less than reference), there will be a wider pulse (i.e. higher duty ratio D) being generated to switches, so that the charging process becomes longer, more power will be passed to output to enhance its power level.

By the circuit waveform, it can be observed that the ratio of between control signal V_c is equal to the duty cycle D. Therefore, the transfer function of pulse width modulator (T_m) can be deduced as

$$T_m(s) = \frac{d}{V_c} = \frac{1}{V_{Tm}}$$ (3.2)

3.4 DESIGN OF CONTROL CIRCUIT FOR KY CONVERTER

From introduction of chapter 2 and previous introduction of this chapter, the transfer functions of the KY converter power stage (T_p), pulse-width modulator (T_m), the feedback network (β) and compensator (T_c), have been mentioned. In order to design a compensator for provide enough phase margin base on its poles and zero as shown in table 3.2, the corresponding value of crossover frequency f_c should be considered first, which is defined as a frequency when the magnitude of loop gain become unity as shown in equation (3.3).

31

$$\left|T_c(j\omega_c) * \beta * T_m * T_p(j\omega_c)\right| = 1 \tag{3.3}$$

Two conditions need to be considered for chose the crossover frequency. Firstly, it's proper to selected a crossover frequency as a range of 1/5 to 1/10 of switching frequency [3.2]. Also, for avoid the effect on LC resonant inside the converter, crossover frequency should be selected at least three times larger than the output resonant frequency.

After understand the restriction of crossover frequency, components values for compensation circuit can be decided. For type III compensator, a separation factor K can be to simplified the design process. Equation for calculate K is shown below, while φ_m represent the required phase to boost for type III compensator. As can be seen in figure 3.4.1, φ_m increase quickly in smaller K, while the increase become slower when the K become higher.

$$K = \left\{\tan\left[\left(\frac{\varphi_m}{4}\right) + 45°\right]\right\}^2 \tag{3.4}$$

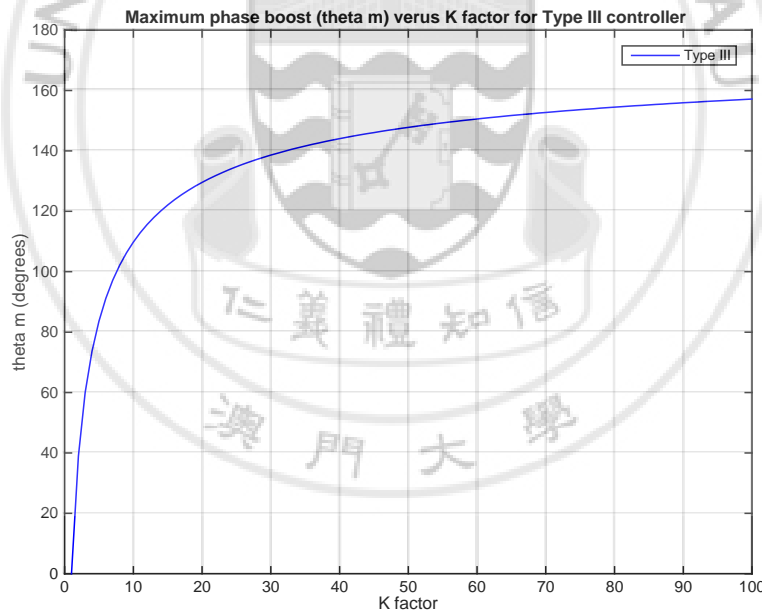
Figure 3.4.1 Plot of maximum phase vs. separation factor K [3.3]

Let the gain and phase at control plants at ω_c be G_p and φ_p, it can be obtained by substitute $s = j\omega_c$ into (2.12). For meet the phase margin PM requirement, we have

$$\varphi_m = PM - \varphi_p - 90° \tag{3.5}$$

After the required gain of compensator $|T_c(j\omega_c)|$ be calculated from (3.3), by selected a resistor R_1, remaining components value can be obtained with the help of K.

$$C_2 = \frac{1}{\omega_c * |T_c(j\omega_c)| * R_1} \tag{3.5}$$

$$C_1 = C_2 * (K - 1) \tag{3.6}$$

$$R_3 = \frac{R_1}{K - 1} \tag{3.7}$$

$$C_3 = \frac{1}{\omega_c * \sqrt{K} * R_3} \tag{3.8}$$

$$R_2 = \frac{\sqrt{K}}{\omega_c * C_1} \tag{3.9}$$

By setting crossover frequency as 2KHz, bases on the parameter setting as previous and equation (2.12) and (2.28), components value for compensator can be determined. In figure 3.4.2 and 3.4.3, bode plot of CCM and DCM in open loop situation and close loop with phase margin in 45°, 60° is shown respectively. Correspondingly, compensator parameters are shown in table 3.3 and 3.4.

PM	K Factor	Resistor			Capacitor		
		$R_1\,(\Omega)$	$R_2\,(\Omega)$	$R_3\,(M\Omega)$	$C_1\,(mF)$	$C_2\,(mF)$	$C_3\,(mF)$
30°	13.8834	50	1127	612.86	0.02	0.26	5.5
45°	25.168	50	809.11	326.7	0.02	0.49	7.67
60°	57.3378	50	523.9	140.15	2.04	1.15	11.84

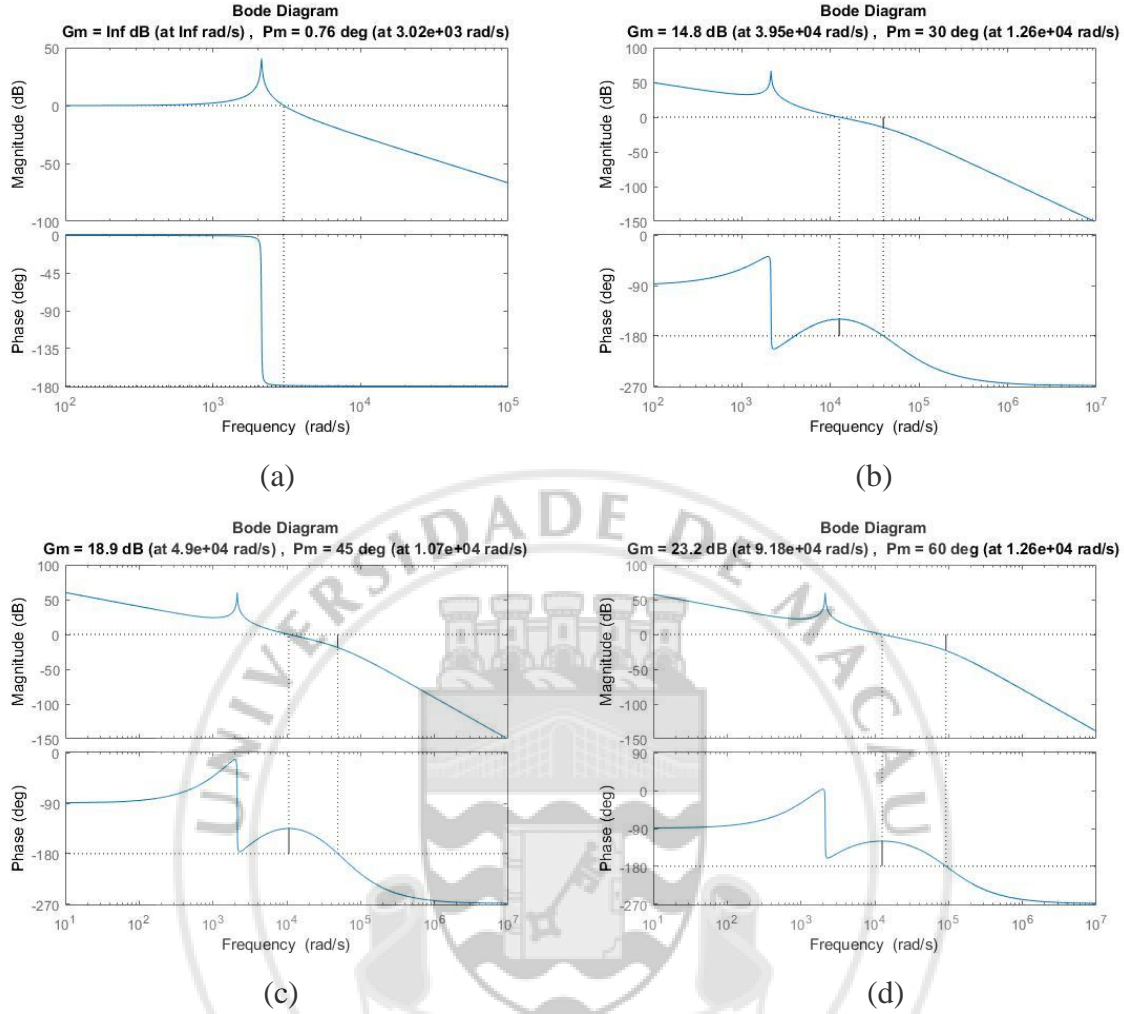Table 3.3 Parameters of compensator be used in simulation for CCM

(a)

(b)

(c)

(d)

Figure 3.4.2 Bode of KY converter in CCM (a) Open loop and close loop for (b) PM = 30°; (c)
PM = 45°; (d) PM = 60°

PM	K Factor	Resistor			Capacitor		
		R_1 (Ω)	R_2 (Ω)	R_3 (GΩ)	C_1 (mF)	C_2 (mF)	C_3 (mF)
30°	2.2158	50	54.13	6.49	1.8	2.19	1.3
45°	2.9657	50	38.73	4.02	1.8	3.54	1.82
60°	4.067	50	29.11	2.58	1.8	5.51	2.42

Table 3.3 Parameters of compensator be used in simulation for DCM

(a)

(b)

(c)

(d)

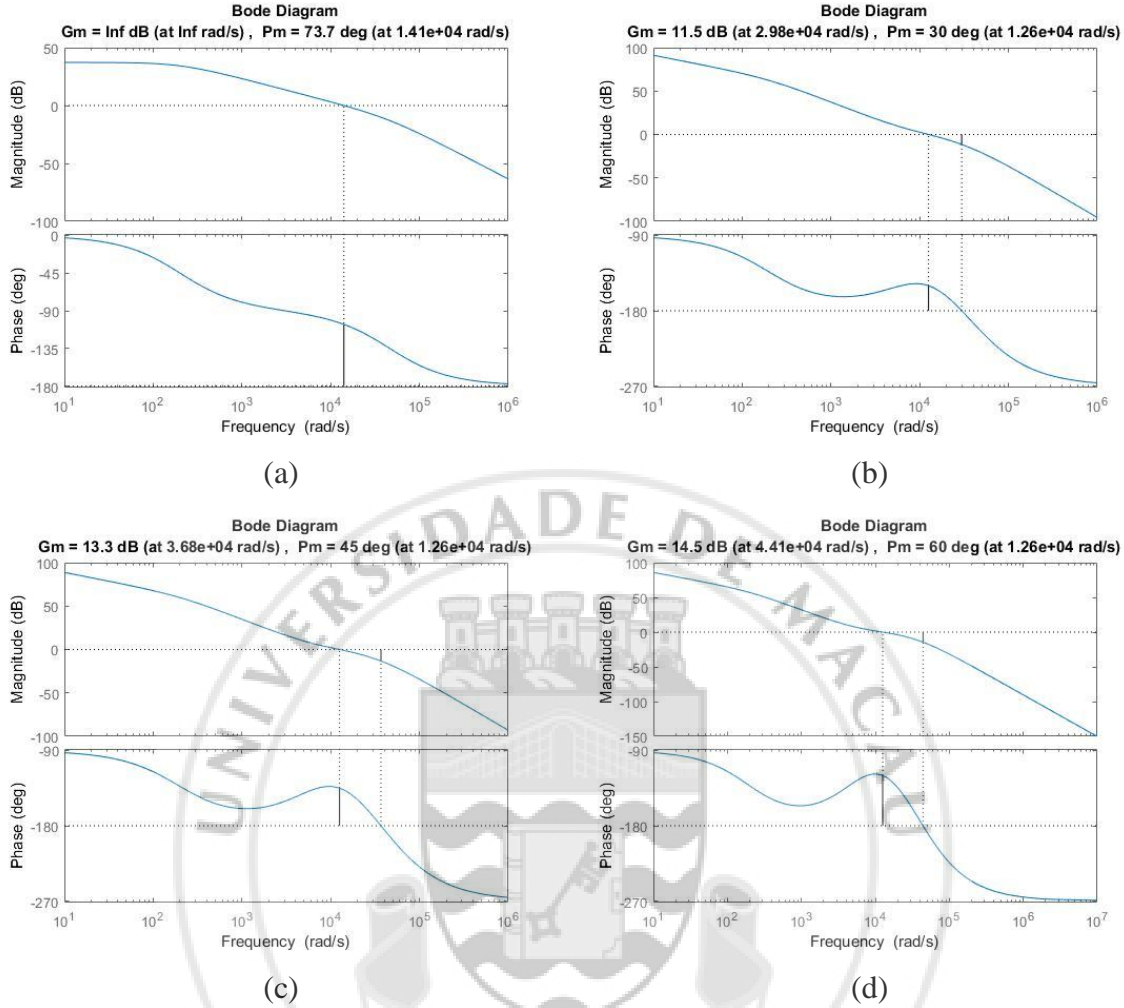Figure 3.4.3 Bode of KY converter in DCM (a) Open loop
and close loop for (b) PM = 30°; (c) PM = 45°; (d) PM = 60°

Thus, simulations base on the components value shown in table 2.3.1 were conducted to check the performance of KY converter in CCM/DCM with 30°/45°/60° phase margin. Noted that the inductance in CCM is changed to 0.5mH instead of 0.12mH in DCM. It is for reduce the boundary current level between CCM/DCM based on equation (2.16), to enable the simulation running in both CCM/DCM in same load condition.

From simulation waveform, inadequate phase margin might lead the system become unstable as represented in figure 3.4.4 (a) for 30° phase margin in CCM. Overall, phase margin in 60° tends to provide lower overshoot level in roughly the same settling time with the other comparators. Thus, design controller being used for experiment will base on the 60° phase margin requirement. During simulation, PI controller information can be obtained from (3.1). The P and I value be used plot following figures is shown in table 3.4.

	Proportional Gain (P)			Integral Gain (I)		
Phase Margin (PM)	30°	45°	60°	30°	45°	60°
DCM	1.72	1.38	0.851	5440	10700	12400
CCM	0.00168	0	0	122	91.5	88.4

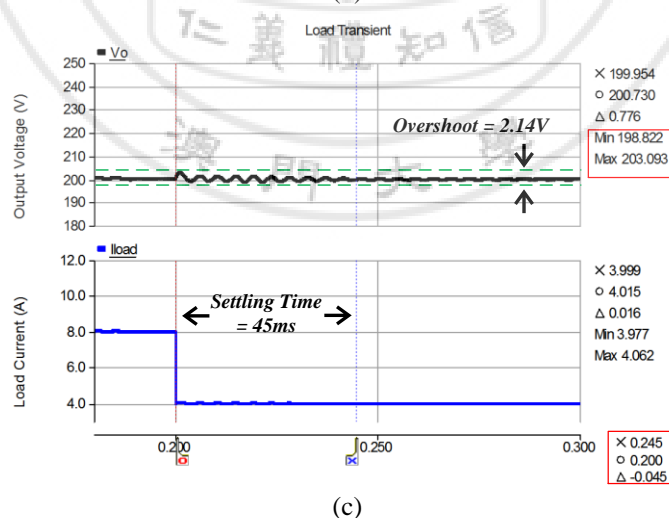Table 3.4 PI parameters for phase margin simulation

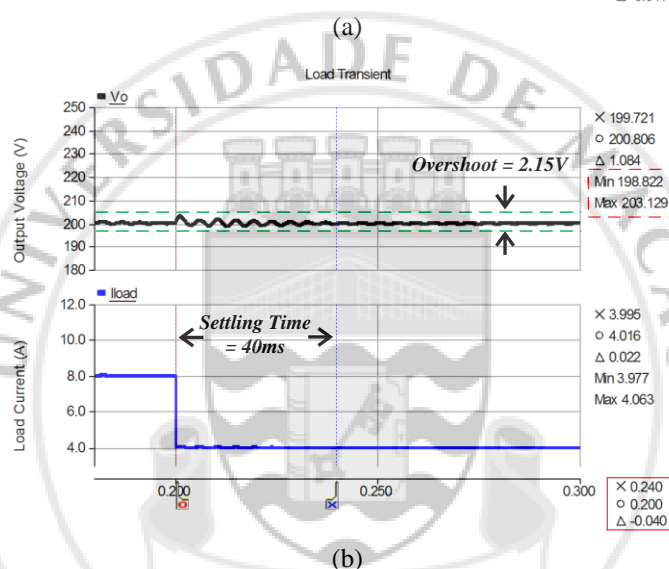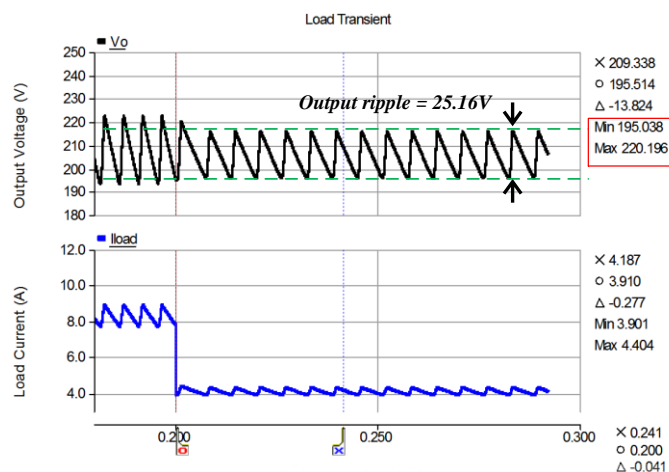Figure 3.4.4 Transient response of KY converter in close loop CCM in phase margin for (a) PM = 30°; (b) PM = 45°; (c) PM = 60°
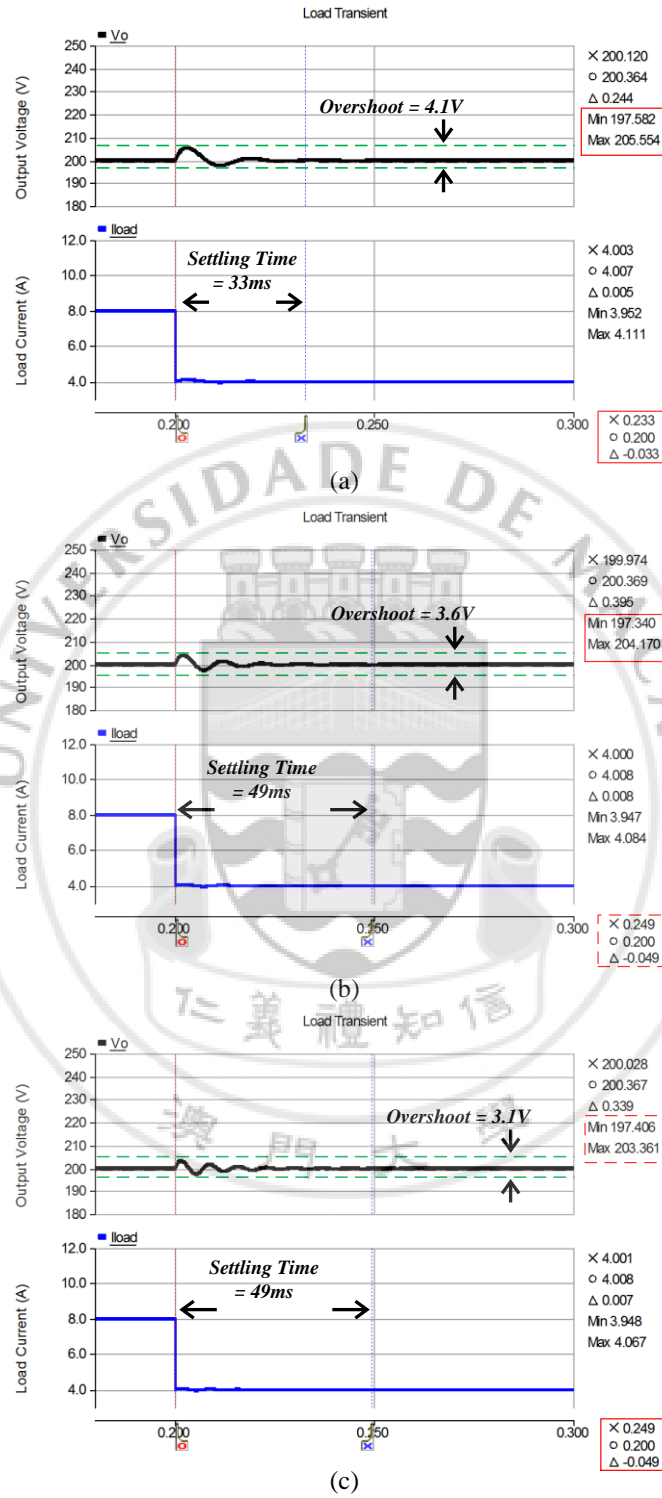
Figure 3.4.4 Transient response of KY converter in close loop DCM in phase margin for (a) PM = 30°; (b) PM = 45°; (c) PM = 60°

In summary, an analog design schematic of KY converter with close-loop compensation is represented in figure 3.4.5.
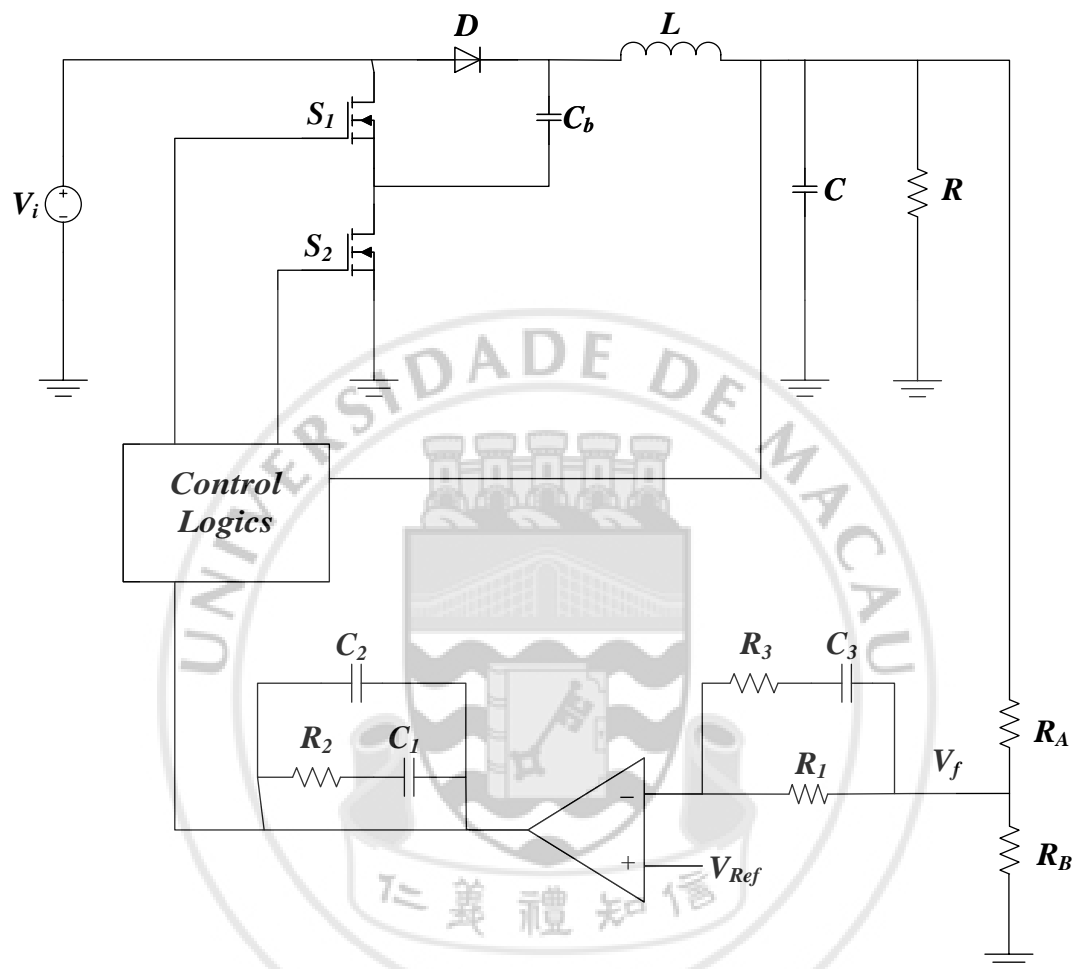

Figure 3.4.5 System structure of KY converter with close loop control

CHAPTER 4: HARDWARE IMPLEMENTATION OF KY CONVERTER

4.1 INTRODUCTION

In this final year project, a hardware circuit is built up to verified the correctness of proposed circuit and control theory. Since the working principle of KY converter have been introduced in chapter 2 and its control theory have been introduced in chapter 3, all techniques are combined and realized in hardware be introduced in this chapter. The overall experimental system was configured as a DC-DC step up converter with close loop control. In practical, overall system function was realized by some extra components include voltage and current transducer, signal conditioning circuit, IGBT driver and digital signal processor (DSP). They are used to perform the same function as theoretical design in chapter 3, which provide higher adjustability for circuit debug. Design and functions of these components will be discussed in sections of this chapter. After that, simulation and experimental result will be shown in comparison with simulation result in next chapter.

4.2 STRUCTURE OF EXPERIMENTAL CIRCUIT

Overall, experimental circuit can be divided into two parts, which are KY converter and related components for sensing, processing and driving the circuit for system work in closed-loop control. Its completed configuration is shown in figure 4.2.1.

As introduced in chapter 1, proposed KY converter is used to step up the voltage from PV Panel and output connected with a DC/AC converter. During the experiment, a controllable DC power supply rating at 600V/17A with self-protection mechanism has been used as the input of KY converter, as a replacement of PV panel. A variable linear load bank has been used as the load of system. Picture of these devices is shown in figure 4.2.2. An extra 3.3mF capacitor is connected in parallel with DC source for to minimize the input voltage fluctuation caused by LC component in circuit, and a Module case circuit breaker (MCCB) which has a current rating in 20A is further connected for further safety concern. Overall, photo of experimental platform is shown in figure 4.2.3.
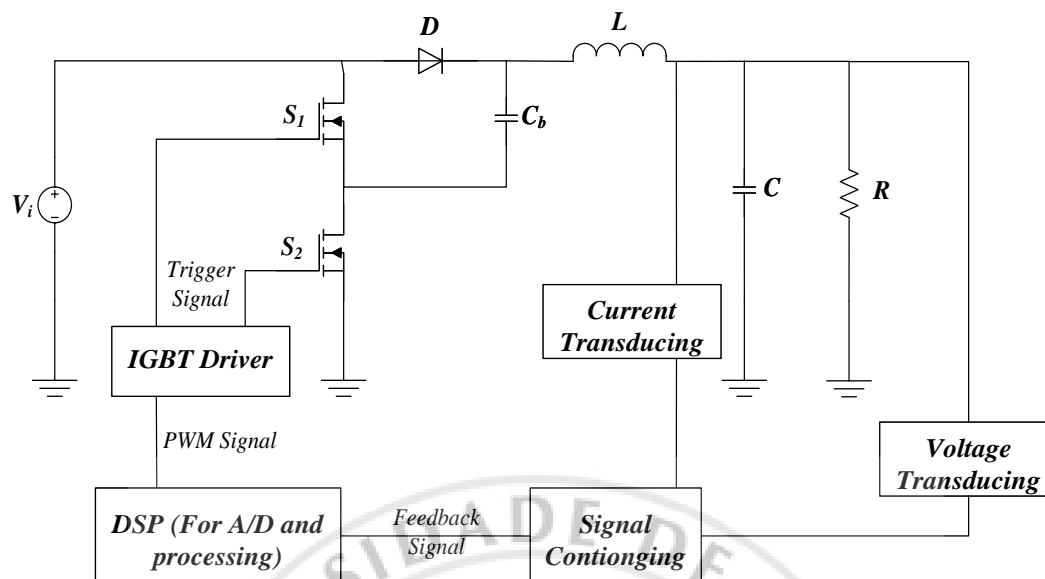
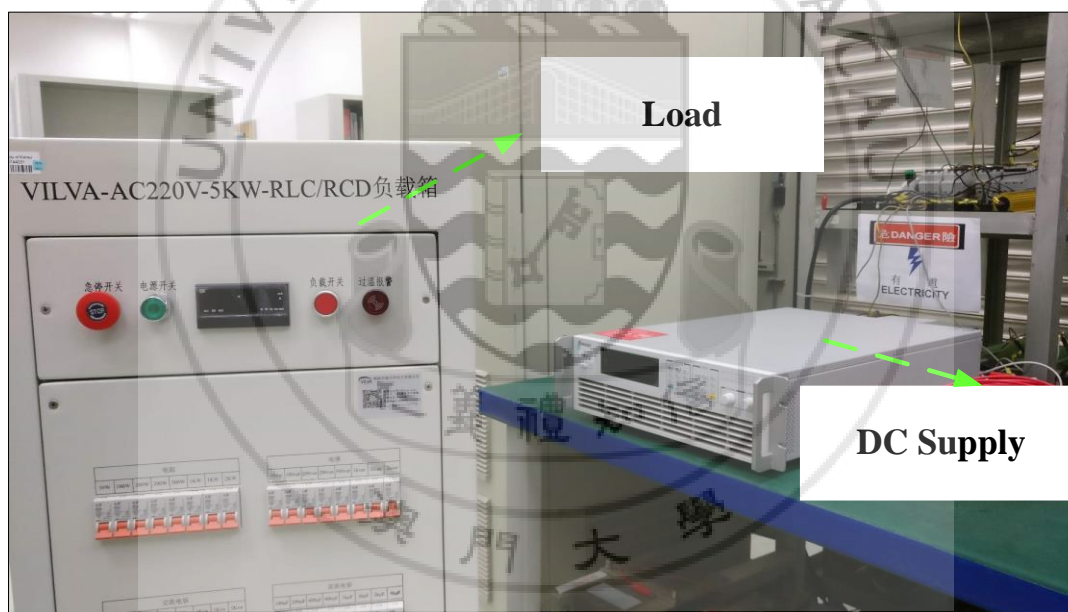Figure 4.2.1 Overall system structure of experimental circuit

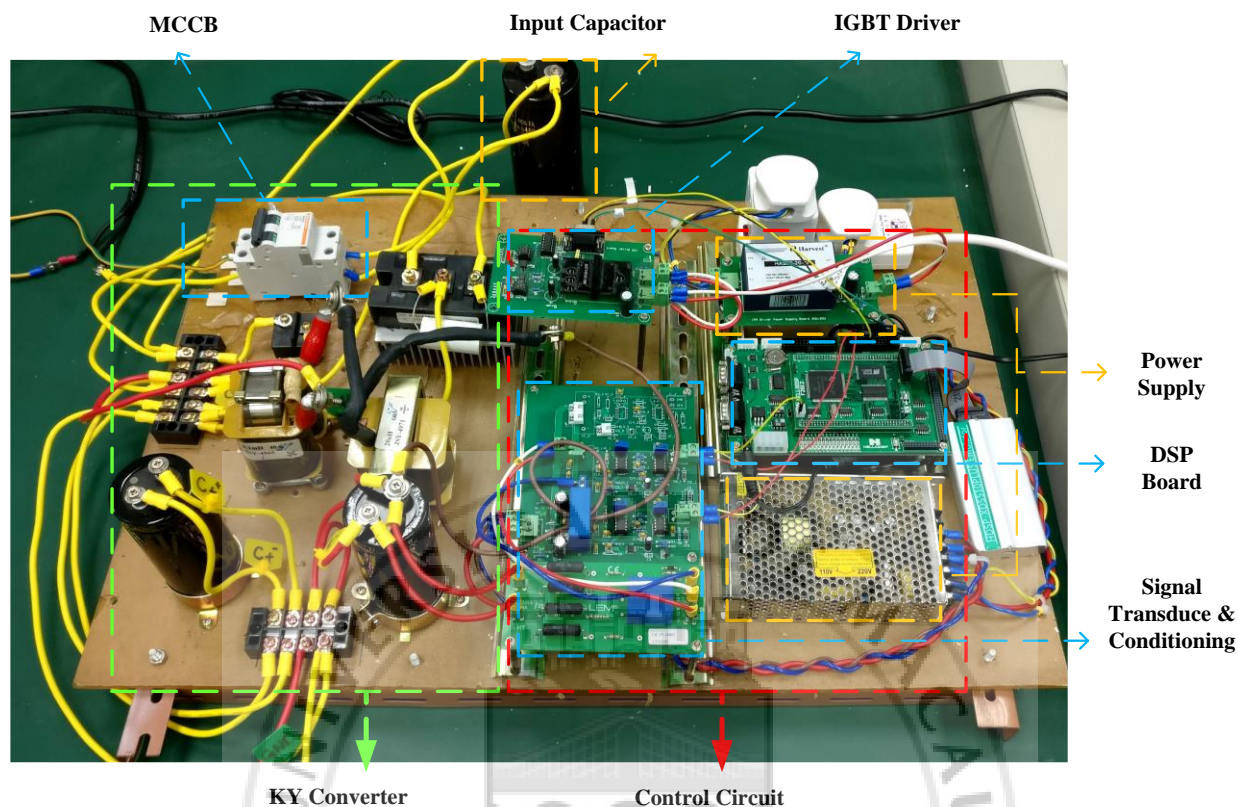Figure 4.2.2 DC power supply and load box

Figure 4.2.3 Hardware of KY converter with closed-loop control

4.3 DESIGN OF EXPERIMENTAL CIRCUIT

4.3.1 SWITCHING DEVICE AND ITS DRIVER

For switched-mode power converter, Metal-Oxide-Semiconductor field effect transistor (MOSFET) and Insulated-Gate Bipolar Transistor (IGBT) are the most popular choice as switching device. MOSFET is characterized as high switching frequency for up to hundred KHz. However, its voltage rating is typically below 200V, which is not suitable for proposed design. In comparison, IGBT has similar merit of low switching losses, low power required for driving as MOSFET. Also, it can work normally in voltage up to kV level, and switching frequency up to 20kHz. For designed output in 200V and 15KHz switching frequency, IGBT shows better compatibility.

In this project, Mitsubishi intelligent power module PM300DSA600 was chosen. It can sustain voltage up to 600V, current up to 300A, and operates in frequency up to 20KHz [4.1]. Figure 4.3.1

shows its appearance and internal circuit diagram. With one package, there are two IGBTs built in with separated control circuits provided for optimum gate drive. Besides, each of them is connected with a freewheeling diode for protection.
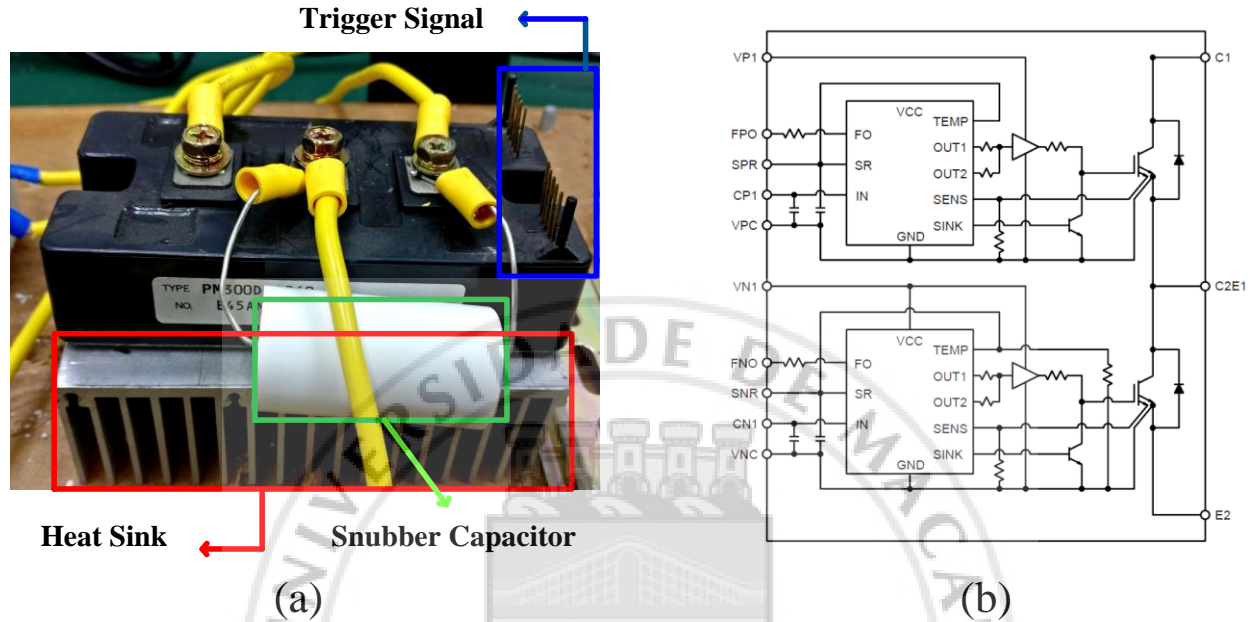
Figure 4.3.1 (a) Photo of PM300DSA600 and (b) its circuit structure [4.1]

In practical, a snubber capacitor is connected between collector port on first IGBT and emitter port of the second. It its used to absorb the suddenly energy increase on switch due to inductor inside the system. As shown in figure 4.3.2, phenomena of voltage spike are improved after the snubber capacitor be connected.

Figure 4.3.2 Eliminated voltage spike on IGBT when snubber is (a) Not applied and (b) Applied

Since the output PWM voltage level from DSP is not enough to trigger the IGBT, an extra driver is required to active the switching function. Schematic of IGBT driver is shown in figure 4.3.3. Here are some considerations of its design base on the DSP I/O requirement:

- The SN74HCT08 is used to protect the I/O of DSP controller. It works as a buffer since the current of the I/O is recommended to within 1.67mA per pin for 3.3 V-tolerance; while the typical working current of HCPL4504 is 16mA.
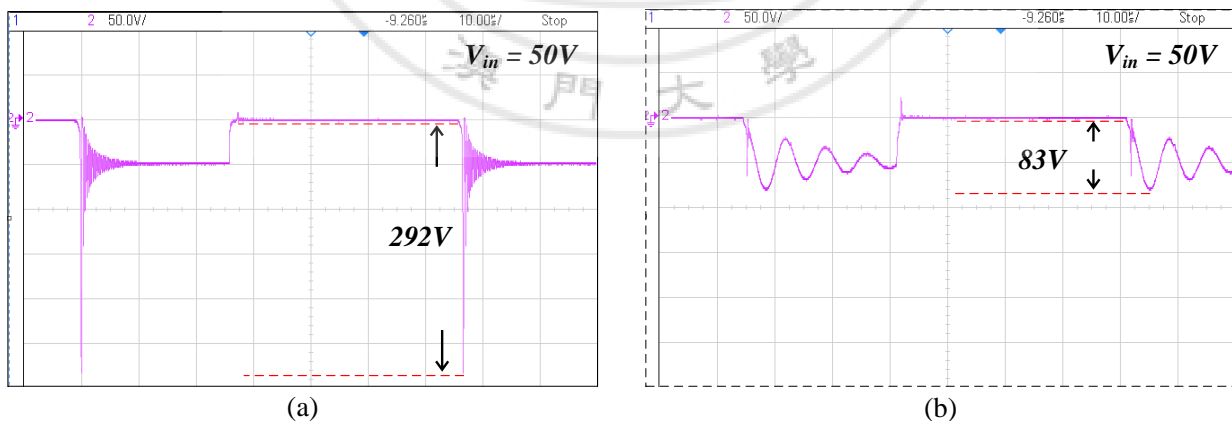
- +VL, R7 and R8 are combined as resistor divider to pull up the signal "FO" and limit the voltage within 3.3V.

- The RC low-pass filter is adopted to filter the noise which could probably be on the fault signal. The selection of R1 should consider the current of controller I/O, "FO" pull up potential and RC low-pass filter loading effect.

The final hardware connection between IGBT and driver is shown in figure 4.3.4.
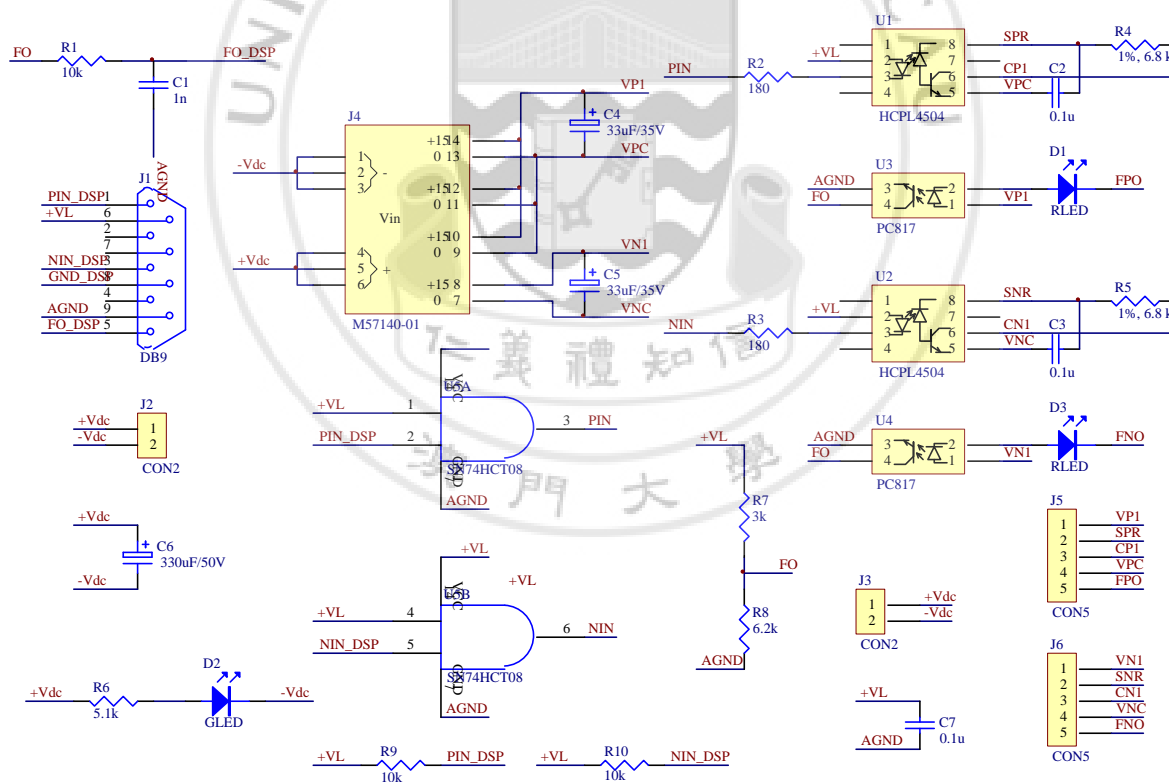
Figure 4.3.3 Schematic of IGBT Driver

IGBT　　　　　　　　　　**IGBT Driver**
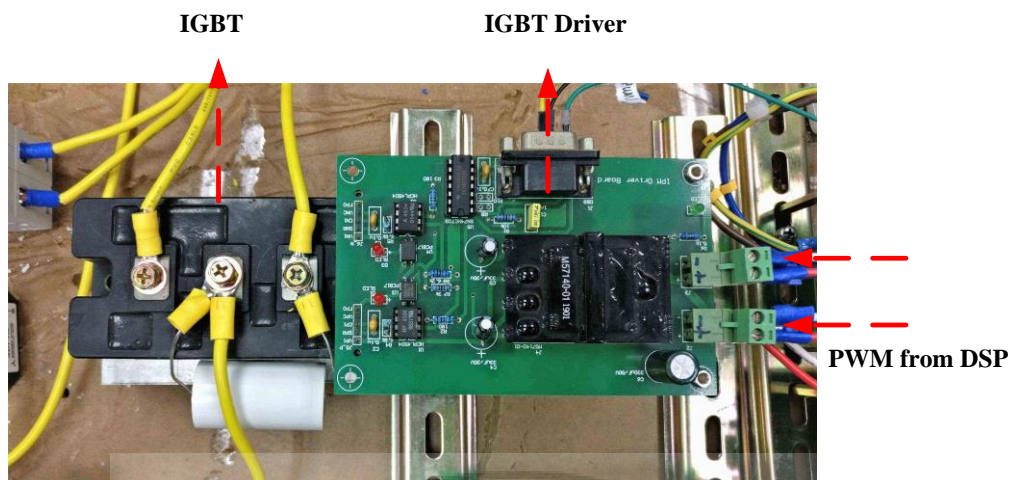
Figure 4.3.4 Connection of IGBT and its driver

PWM from DSP

4.3.2 SIGNAL TRANSDUCING AND CONDTIONING CIRCUIT

For proposed design, one voltage signal (output voltage) and one current signal (inductor current) need to be sensed for control logics. Each of them require specific transducing circuit, which will be discussed in coming sections.

4.3.2.1 CURRENT TRANSDUCER

Current signal is sensed by a current transducer LA55-P as shown in figure 4.3.5. By retrieved its specification from datasheet, it can sense primary nominal root mean square current in maximum of 50A and provides good linearity and frequency bandwidth [4.2]. For a circuit maximally has 20A current flowing (restricted by MCCB), it shows good compatibility for this project.

（a）　　　　　　　　　　(b)

Figure 4.3.5 (a) Drawing of current transducer and its (b) internal connection [4.2]

For a current signal conducting in specific wire, this transducer will let the wire go through the void area in middle. Base on hall effect, primary current I_p pass through transducer will produce a

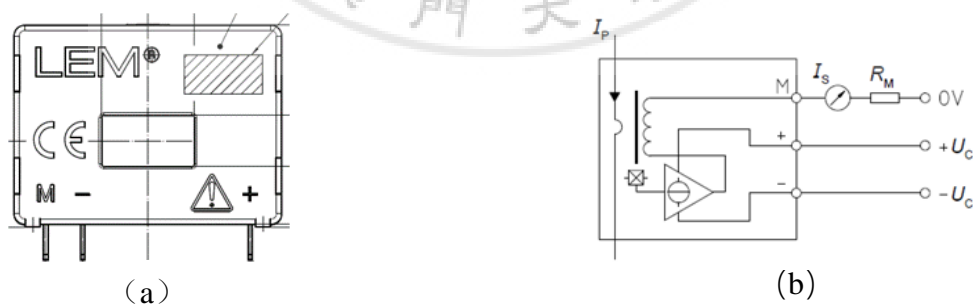current signal I_{s1} in secondary side. This model provides a conversion in 1000:1 from primary to secondary. To increase sensitivity of current sensing, conduction wire was winding up twice when it passes through the transducer, which means the amount of current be sensed is double as actual value. Relationship between primary and secondary current is shown in equation (4.1).

$$I_s = \frac{1}{500} I_p \qquad (4.1)$$

4.3.2.2 VOLTAGE TRANSDUCER

Schematic of voltage transducer LV 25-400 is shown in figure 4.3.6. It allows a primary nominal rms voltage V_{PM} in range of 0 to ±400V [4.3]. For measure the output voltage in proposed design as 200V, it is enough even considering the overshoot level.

(a)

(b)

Figure 4.3.6 (a) Drawing of voltage transducer and its (b) internal connection [4.3]
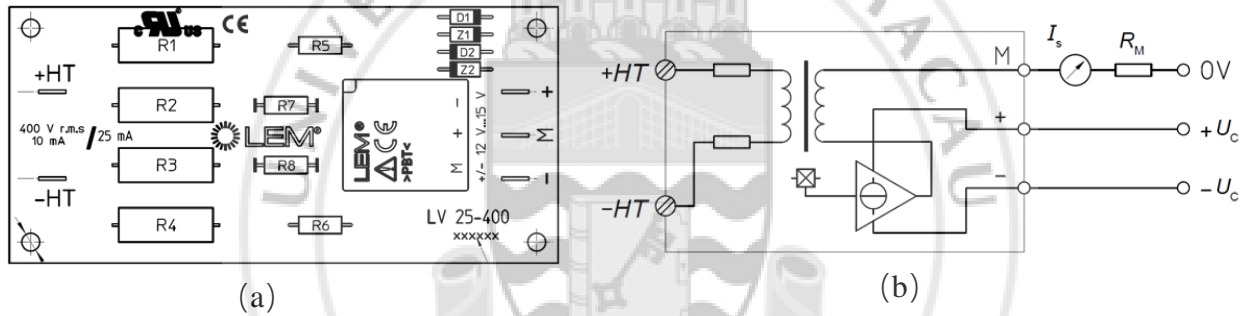
Transduce of voltage signal has similar principle as current transducing. By connect +HT/-HT terminal for primary signal V_{PM} with various resistors integrated inside the transducer board, it will produce a current flow in primary side. By hall effect, it will cause a current signal I_{s2} in secondary side. Relationship between V_{PM} and I_{s2} is shown in equation (4.2).

$$I_{S2} = \frac{1}{1600} V_{PM} \qquad (4.2)$$

4.3.2.3 SIGNAL CONDITIONING CIRCUIT

Before the transduced signals pass to DSP, they will pass through a conditioning circuit, which is used to adjust signal's gain and filter noise. In practical, signal being sensed by transducer will always contain some interference, which may dramatically affect the correctness of feedback value,

then leads the system become uncontrollable. Signal conditioning circuits are able to transfer the signal into a proper level for input requirement of DSP, also can reduce the noise for improve the accuracy of control. Figure 4.3.7 shows the schematic of signal conditioning circuit.
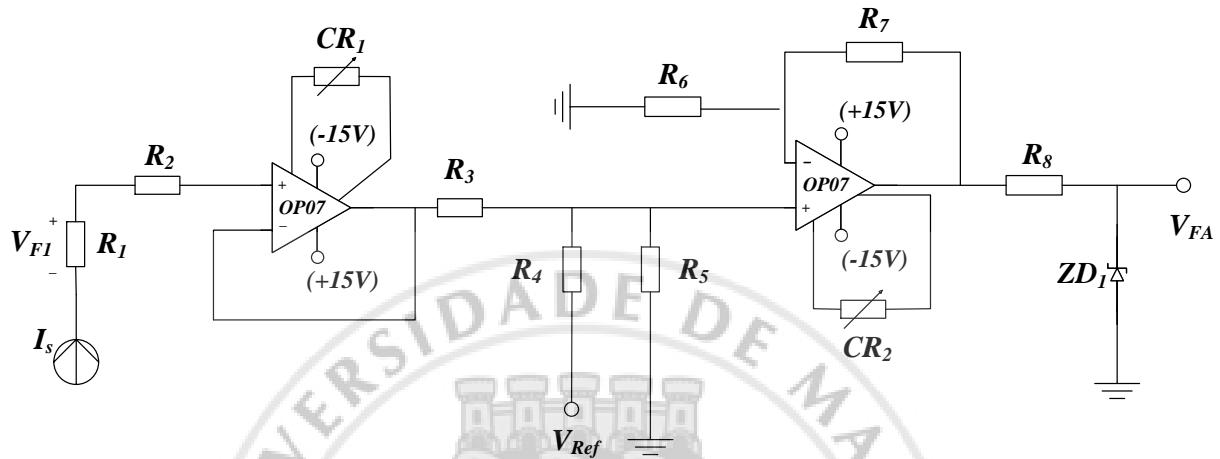
Figure 4.3.7 Schematic of signal conditioning circuit

Within the circuit, two operational amplifiers OP07 will be used. Figure 4.3.8 shows the simplified schematic and pins function of OP07. It requires power supply V_{CC} in range of ±3V to ±18V and typically work in input ranging in ±14V [4.4]. Each operational amplifier is connected with a variable resistor for input offset voltage adjustment. After input current signal I_s from transducers being transform to a voltage signal V_{F1} by R_1, it will pass through a voltage follower formed up by R_2 and the first Op-Amp. It is used as a unity gain buffer to draws high impedance on the load side for minimize the loading effect.

Pin	Description
OFFSET N1	External input offset voltage adjustment
OFFSET N2	
VCC+	Positive Supply
VCC-	Negative Supply
IN+	Inverting input
IN-	Noninverting input
OUT	Output

Figure 4.3.8 Simplified schematic of OP07 and its pin's function [4.4]

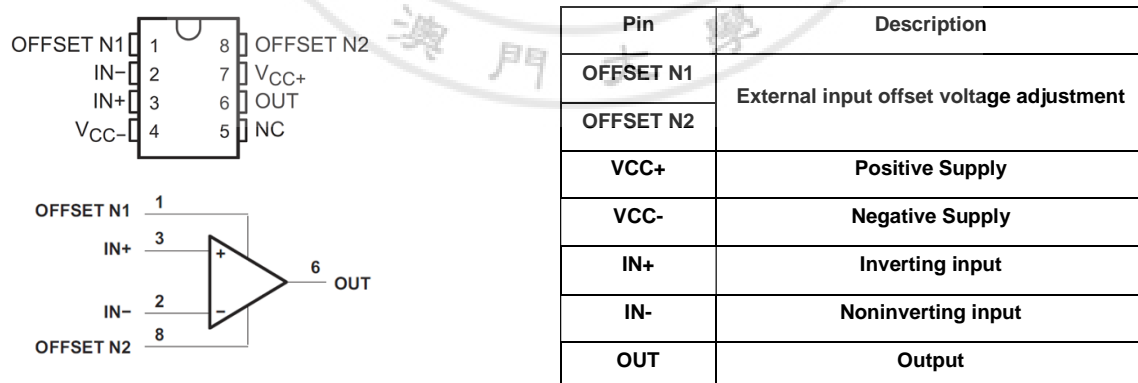The second amplifier is used to normalized the voltage level, while the selection of resistors is based on the input/output specification of Op-amp, transducers and DSP. Based on datasheet, their rating value is given in table 4.1.

Model	LA55-P	LV 25-400	OP07	TMS320F2812
Input Rating	50A	400V/10mA	±14V	0 – 3.3V
Output Rating	25mA	25mA		

Table 4.1 Components rating [4.2] - [4.5]

Besides, a reference voltage in +3V is provided by REF5030 as offset for feedback signal [4.6]. It's for increase the resolution of A/D conversion in low voltage level. Base on the schematic, a transfer relation between input I_s from transducer and output V_{FA} to DSP can be described as equation (4.3).

$$V_{out} = \frac{R_6 + R_7}{R_6}\left(\frac{R_3 R_5}{R_3 R_4 + R_3 R_5 + R_4 R_5}V_{ref} + \frac{R_4 R_5}{R_3 R_4 + R_3 R_5 + R_4 R_5}V_{F1}\right) \qquad (4.3)$$

Consider the current flow and possible peak output voltage level, saturation level for output voltage feedback is 225V and 9.85A for inductor current. After the feedback exceed the saturation level, a Zener diode Z_{D1} is placed before connect to A/D port to limit the feedback signal to DSP below 3.3V. Based on above information, resistor value for R_1 to R_8 were selected as shown in table 4.2 and 4.3. Hardware connection of transducers and signal conditioning circuit is shown in figure 4.3.9.

R_1 (Ω)	R_2 (KΩ)	R_3 (KΩ)	R_4 (KΩ)	R_5 (KΩ)	R_6 (KΩ)	R_7 (KΩ)	R_8 (Ω)
180	10	1	6.8	2	15	10	100

Table 4.2 Resistance for output voltage signal condition circuit

R_1 (Ω)	R_2 (KΩ)	R_3 (KΩ)	R_4 (KΩ)	R_5 (KΩ)	R_6 (KΩ)	R_7 (KΩ)	R_8 (Ω)
180	10	1	6.8	2	18	4.3	100

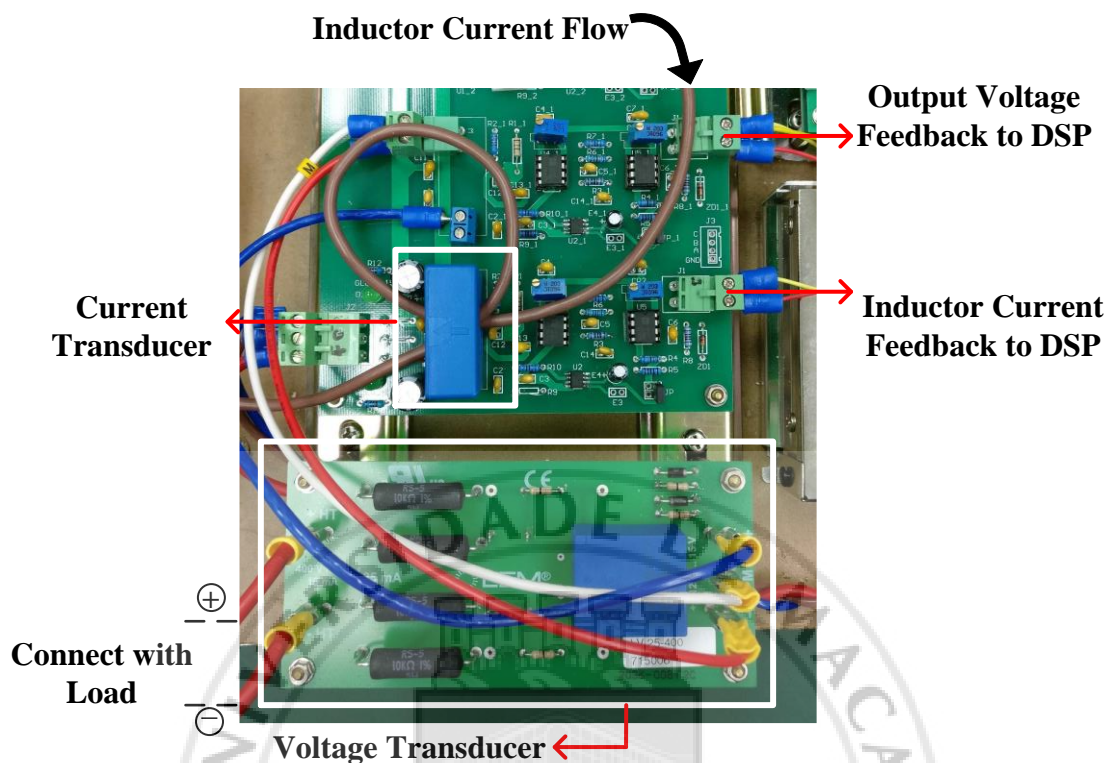Table 4.3 Resistance for inductor current signal condition circuit

Figure 4.3.9 Connection of transducers and signal conditioning circuit

4.3.3 DIGITAL SIGNAL PROCESSING BOARD

The DSP board is based on a 32-bit fix point digital signal processor TMS320F2812 in clock frequency of 150MHz. It is widely used in power application included motor/machine control, converter/inverter control, etc. By sample the feedback signal on A/D module into a digital signal, it will be processed by designed algorithm for a PWM signal generated to IGBT driver board. It combines the function of control logics and compensator as the analog design in chapter 3.

Moreover, for realize a PID control on proposed system, it shows higher performance and flexibility for design. In general, the program flow chart of DSP is shown in figure 4.3.10. In general, the functions of this controller are:

- Converter the feedback signal to digital through A/D module;
- Implement algorithm on A/D result;
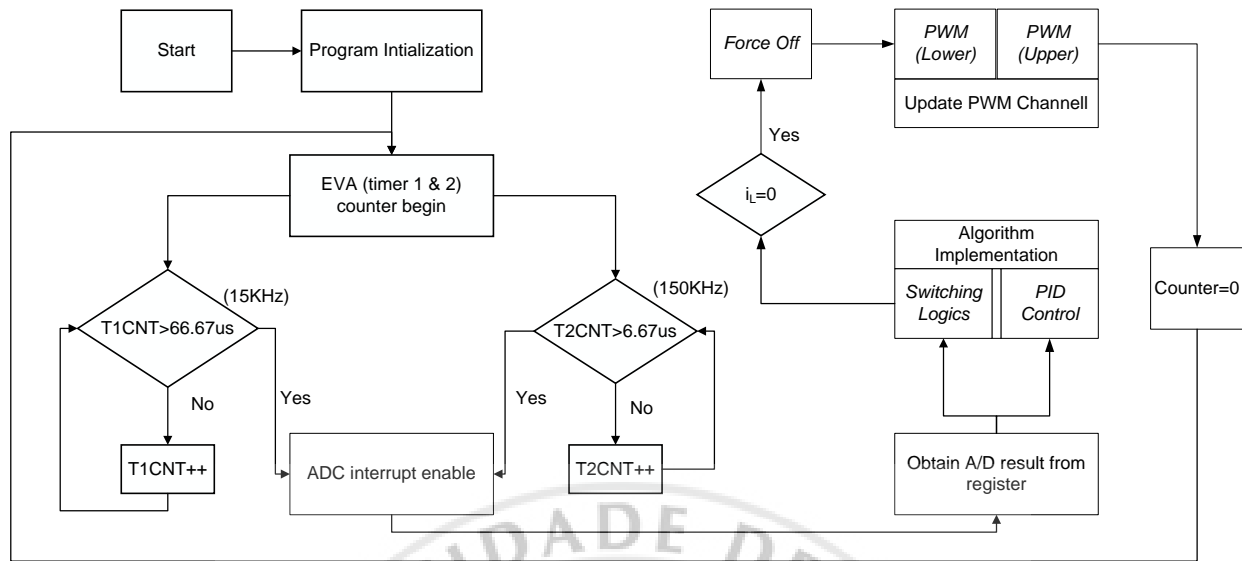- Generated PWM signals trigger signals

Figure 4.3.10 Program flow chart in DSP

4.3.3.1 ANALOG TO DIGITAL MODULE

The A/D module in F2812 is a 12-bit module with fast conversion rate of 80ns at 25 MHz clock. Its block diagram is shown in figure 4.3.11. Inside, each of the event manager EVA and EVB provides 8 channel and two timers. Timer is used to define the sampling rate of A/D module. Here, 2 channel of signals are converted into digital values. For 15KHz switching frequency in proposed KY converter, Timer 1 of EVA is set as 15 KHz for output voltage feedback will be converted on the first channel by timer 1 of EVA which is set as 15 KHz to updated the PWM of each cycle. Timer 2 for the second channel of inductor current feedback is set as 150 KHz since it is used to detect when inductor current reach zero in each switching cycle.
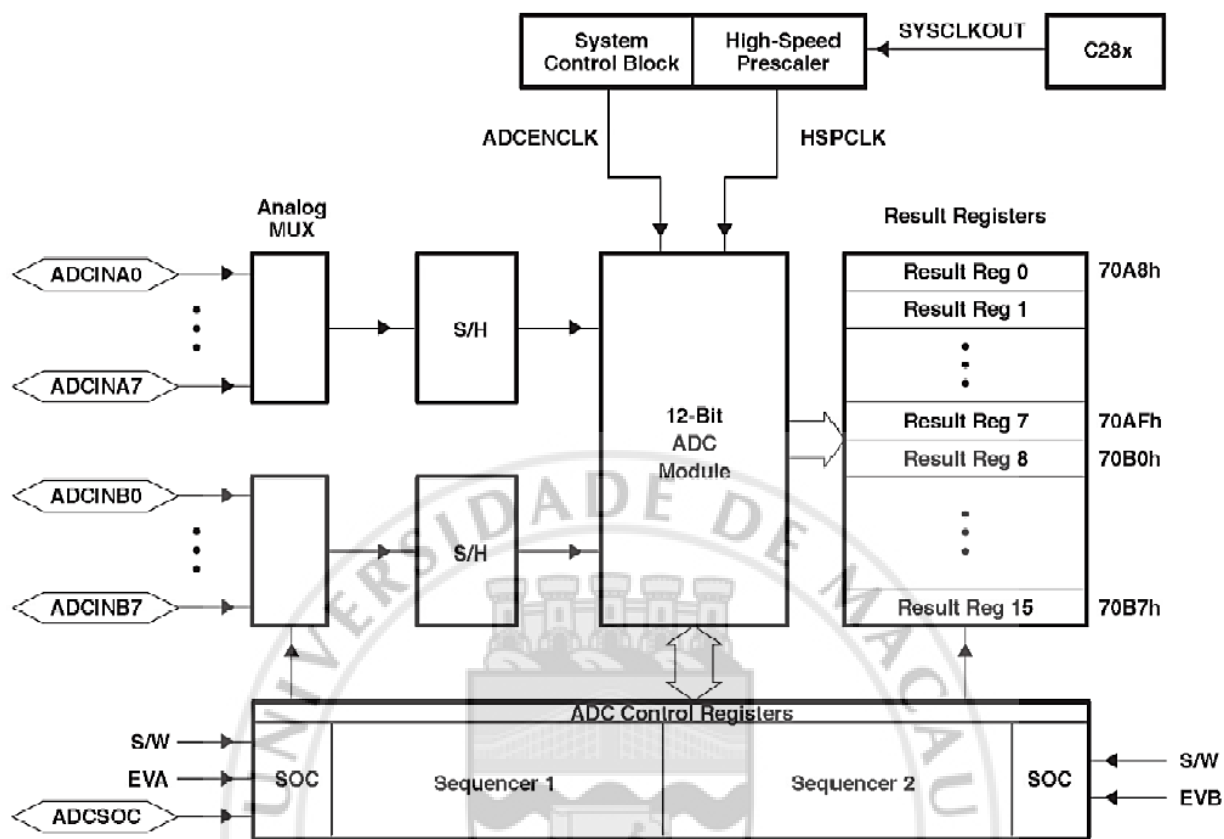
Figure 4.3.11 Block diagram of A/D module in F2812 [4.5]

After feedback signal pass through the sample/hold circuit and be stored into the register, it need to be normalized to analog value for ease of calculation. For a 12-bit A/D module, there is a liner relationship between digital and feedback value is shown as the blue line in figure 4.3.12. In practical, the relationship has slightly shift from the ideal. For further eliminate the mismatch, A/D is further calibrate by obtained various output digital in different feedback voltage. It can be observed that there is a 1.013 offset gain and 0.02V offset for the feedback voltage sensed in DSP. Finally, relationship between digital value and feedback from transducer is shown in (4.4).

$$\text{Digital Value} = 4095 \times \frac{(Analog\ feedback\ voltage * 1.013 - 0.02) - ADCLO}{3} \tag{4.4}$$
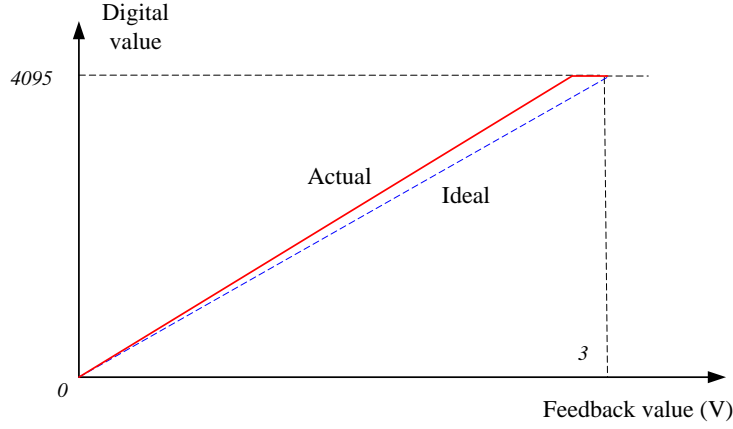
Figure 4.3.12 Feedback value vs. digital value in DSP

4.3.3.2 PWM SIGNAL GENERATION

Generation of PWM signal in DSP is based on compare logic. By setting value TxPR for timer Tx, timer counter TxCNT will repeatedly increase from 0 to TxPR. In logic as shown in figure 4.3.13, relatively, relationship among TxCNT, CMPRx, PWM signal PWMx can be represented by (4.5).

$$\begin{cases} TxCNT > CMPRx \\ TxCNT \le CMPRx \end{cases} \rightarrow \begin{cases} PWMx = 1, PWM(x+1) = 0 \\ PWMx = 0, PWM(x+1) = 1 \end{cases} \tag{4.5}$$

Figure 4.3.13 PWM compare logic of DSP

Counter is based high speed clock HSPCLK = 37.5MHz, therefore, frequency of PWM signal can be represent as (4.6). For the project, T1PR is set as 2499 to provide a 15KHz PWM signal. Base on the information of IGBT's datasheet [4.1], a dead band t_{db} is set as 4.27μs to ensure the switch function properly.
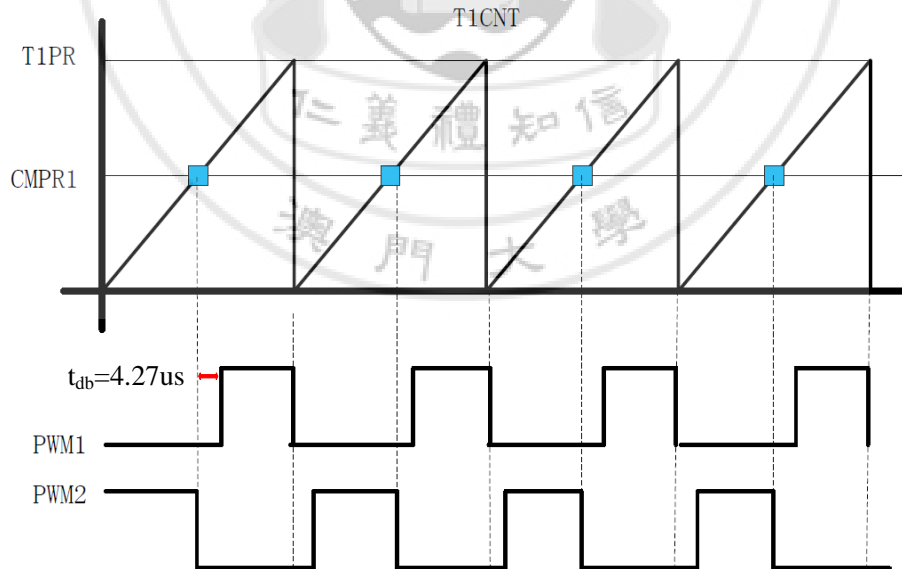
$$f_{pwm} = \frac{HSPCLK}{TxPR + 1} \tag{4.6}$$

4.3.4 REALIZATION OF PID CONTROL IN DSP

For analog PID controller, there is a general form to represent the proportional gain K_p, integral gain K_i and derivative gain K_d value as (4.7). Since the transfer function of analog controller already be deducted as (3.1), corresponding gain value can be retrieved.

$$G_c(s) = K_p + \frac{K_i}{s} + K_d s \tag{4.7}$$

$$G_c(t) = K_p e(t) + K_i \int e(t) \, dt + \frac{K_d de(t)}{dt} \tag{4.8}$$

In time domain, PID controller is implemented using (4.8). For a digital processor, it need to be transformed into discrete time domain to perform integration and differentiation by numerical calculation. Among various approach to obtain a discrete time equivalent PID controller, backward difference method is one of the most used since it occupies relatively simpler calculation [4.7]. By using backward difference method, a numerical integrator and differentiator can be representing as (4.9). T represent the sampling period. Therefore, transfer function of a digital PID controller is shown in (4.10).

$$\begin{cases} t \approx kT, k = 0,1,2, \dots \\ \int_0^t e(t)dt \approx T \sum_{j=0}^{k} e(jT) = T \sum_{j=0}^{k} e(j) \\ \frac{de(t)}{dt} \approx \frac{e(kT) - e[(k-1)T]}{T} = \frac{e_k - e_{k-1}}{T} \end{cases} \tag{4.9}$$

$$u[k] = K_p e[k] + K_i \sum_{j=0}^{k} e[j] + K_d(e[k] - e[k-1]) \tag{4.10}$$

In (4.10), u[k] represent the k_{th} error on calculation result. In DSP F2812, this value should be assigned to CMPx as mentioned in previous section, which is used for compare with counter signal and generate corresponding PWM signal. For each calculation, error e[k] is equals to the subtraction between reference KY converter output voltage V_{ref} and feedback voltage value on DSP (For ease of calculation, A/D convert result will be first normalized to actual value by equation (4.3) and (4.4)). Integral control will accumulate error of each period of calculation, differential control is based on the difference on previous calculated difference and present calculated difference. Indeed, they are the same as root concept on integration and differentiation as mathematical tools. After properly set up the algorithm, by input different K_p, K_i, K_d and V_{ref}, system can run with DSP act as a PID controller to tracking a set reference level.
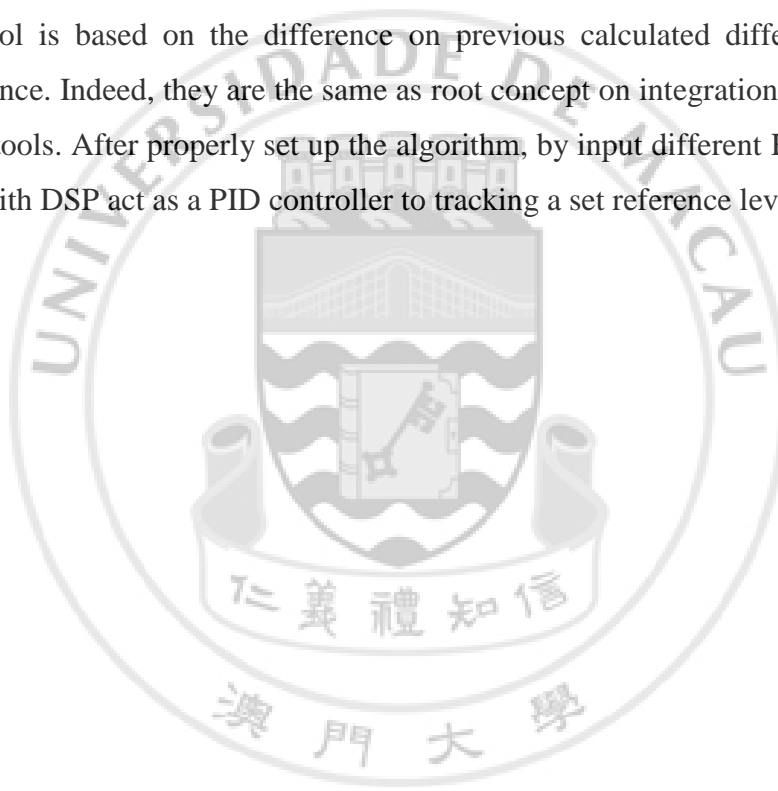
CHAPTER 5: SIMULATION AND EXPERIMENTAL RESULT OF KY CONVERTER

5.1 INTRODUCTION

For verified the validity of theoretical analysis of KY converter in Continuous Conduction Mode (CCM) and Discontinuous Conduction Mode (DCM) and evaluate the performance of closed-loop control circuit, several simulations and experimental tests were conducted. Simulation results were carried out by using PSCAD/EMTDC, which is widely used in power engineering field. In comparison, experiments based on the same component's parameter as simulation were conducted on the hardware be introduced in previous chapter. Selection of KY converter component was based on the theoretical analysis in chapter 2.

System parameters	Physical Values
Input Voltage (V)	120-150V
Output Voltage (V)	180-200V
Inductor	0.12mH (DCM)
	0.22mH (CCM)
	0.5mH (CCM)
Output Capacitor	1mF
Flying Capacitor	1mF
Switching Frequency	15kHz
Load Resistance	25-100Ω

Table 5.1.1 KY converter parameters for simulation and experiment

As shown in table 5.1.1, parameters for CCM and DCM was only different in inductor value. Base on previous analysis, when the system is working below certain boundary output current level, circuit will work in DCM. Since the system was primarily designed for work in DCM for a boundary current in 8A, there will be a safety concern and equipment limitation for the

experimental test in CCM. For CCM, inductance was chosen as 0.22mH for small load condition, and 0.5mH for heavy load condition to made the experimental test became achievable.

5.2 SIMULATION AND EXPERIMENTAL RESULT IN OPEN LOOP

Since operation in DCM requires feedback signal on inductor current to adjust the trigger signal of power switch, KY converter will only work in open loop during CCM. Output voltage is variate by change the fixed duty ratio D base on equation (2.12). As reflection, figure 5.2.1 shows waveform of output voltage in different level along with switch signal. A pulse width will be wider for a higher duty ratio be given, result in higher output voltage.
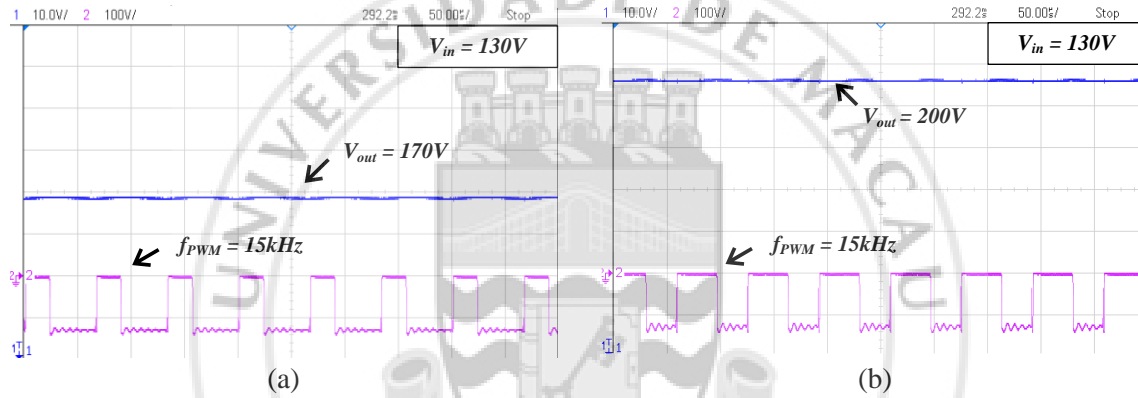

Figure 5.2.1 (a) Waveform under input/output of 130V/170V at 4A load current; (b) Waveform under input/output of 130V/200V at 4A load current;

During CCM, inductor current will not lower than zero and perform as a triangular wave base on theoretical analysis. In figure 5.2.2, waveform on inductor current and output voltage from simulation and experiment is shown where D = 50%. From equation (2.6), output voltage should be equals to 195V. Comprehensively, error simulation/experimental result shows 0.09% / 0.51% in compare with theoretical result is shown in table 5.1 Error in different duty ratio from hardware and software have not exceed 0.62% as test, which can be considered as the theory of KY converter in CCM be proved.

Duty Ratio	0.3	0.4	0.5	0.6	0.7
Simulation	0.08%	0.13%	0.09%	0.09%	0.1%
Experiment	0.62%	0.58%	0.51%	0.49%	0.54%

Table 5.1 Output voltage error among theoretical and simulation/experimental result of KY converter in CCM
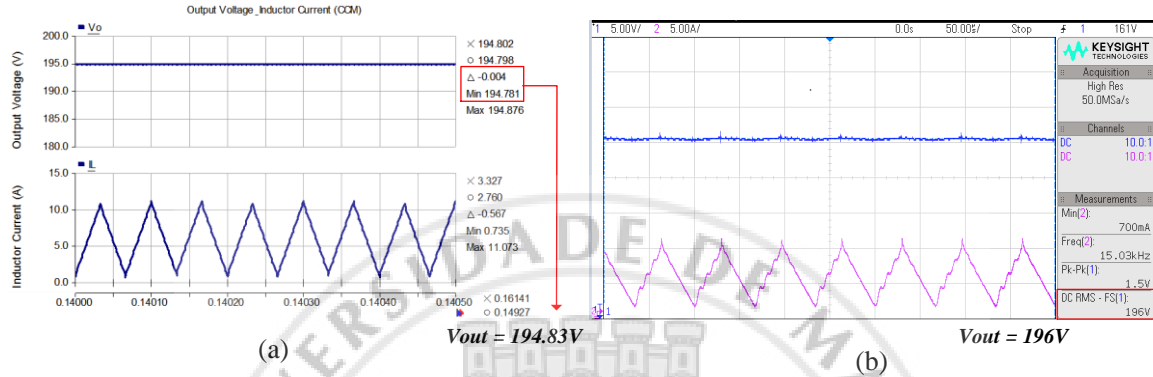

(a)   *Vout = 194.83V*   *Vout = 196V*   (b)

Figure 5.2.2 (a) Simulation result and (b) Experimental result of KY converter in CCM for expected output voltage in 195V

5.3 KY CONVERTER IN CCM WITH CLOSE LOOP CONTROL

System performance can be improved by process output feedback signal to modulate switching signal. Base on the technique introduced in chapter 4, a proportional gain $K_p = 0.125$ was applied to the PID control algorithm inside the DSP to realize overall system's phase margin in 60 degree. For input voltage in 130V and reference output voltage set as 200V, system shows its ability to track the setting value. As reference, figure 5.3.1 illustrates the change in load voltage when load current variate between 4A and 5A. In comparison, close loop transient response from simulation and experiment in same condition is shown in figure 5.3.2 and 5.3.3. With a small change in load condition, present KY converter shows is ability to track the setting value.
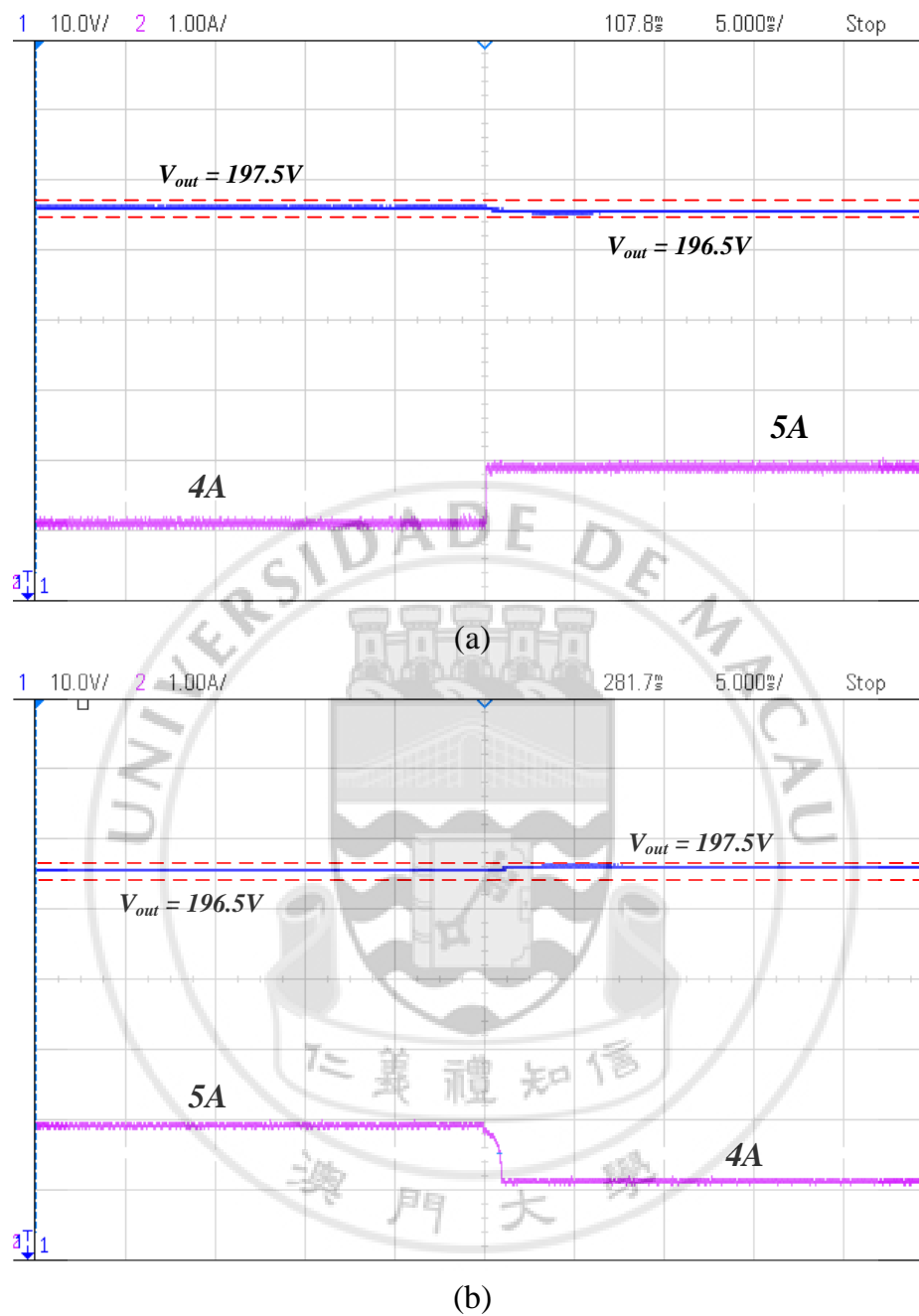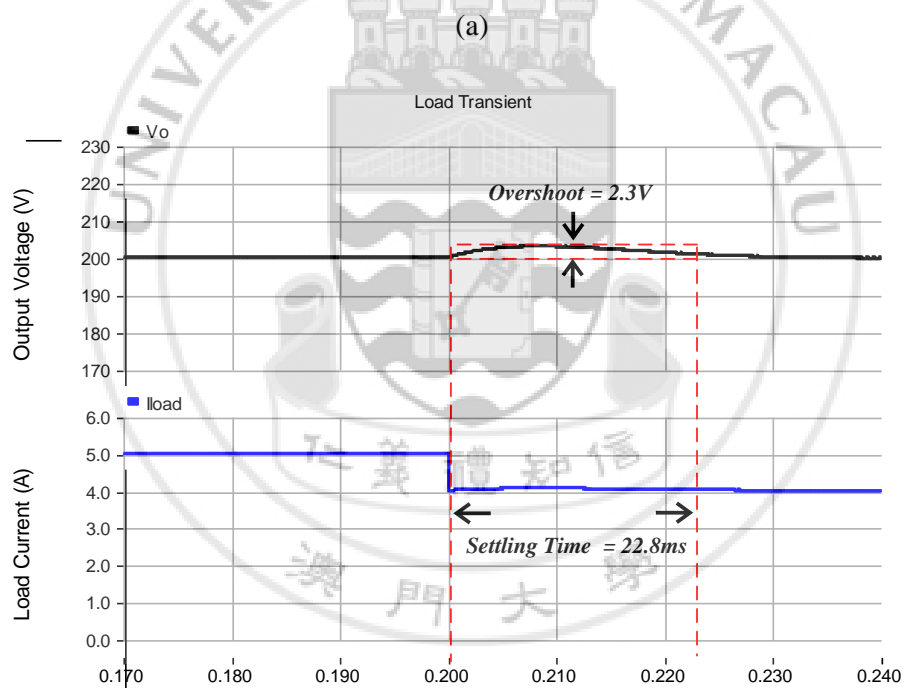
Figure 5.3.1 Output voltage drop in open loop when load current change (a) from 4A to 5A and (b) from 5A to 4A

(a)
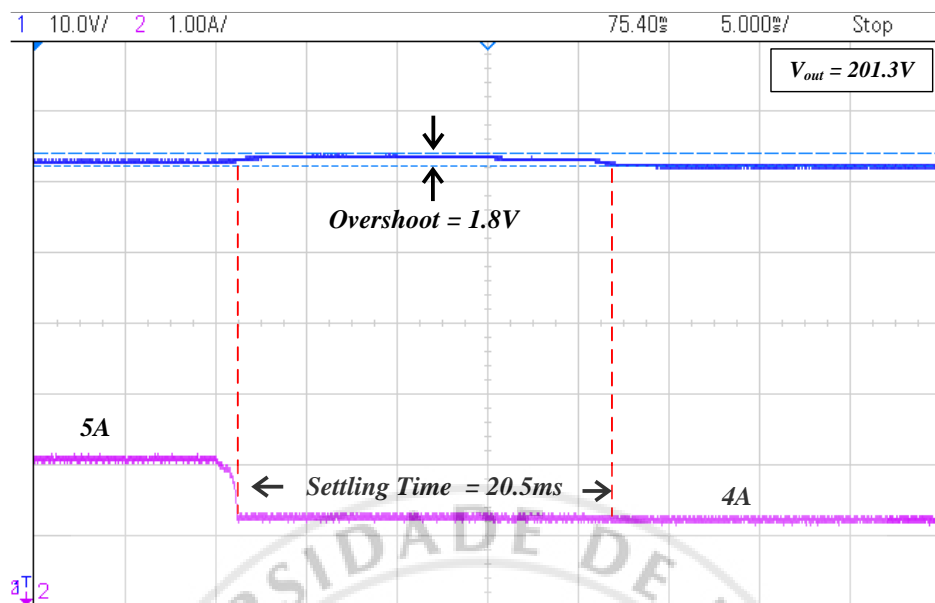
(b)

Figure 5.3.2 (a) Experiment and (b) Simulation result of close-loop load transient when load change from 5A to 4A

(a)

(b)

Figure 5.3.3 (a) Experiment and (b) Simulation result of close-loop load transient when load change from 4A to 5A

To observed transient response in larger change of load, bases on (2.16), inductor with 500µH inductance was set in the circuit to extend the CCM region. Hence, load transient from 2A to 6A

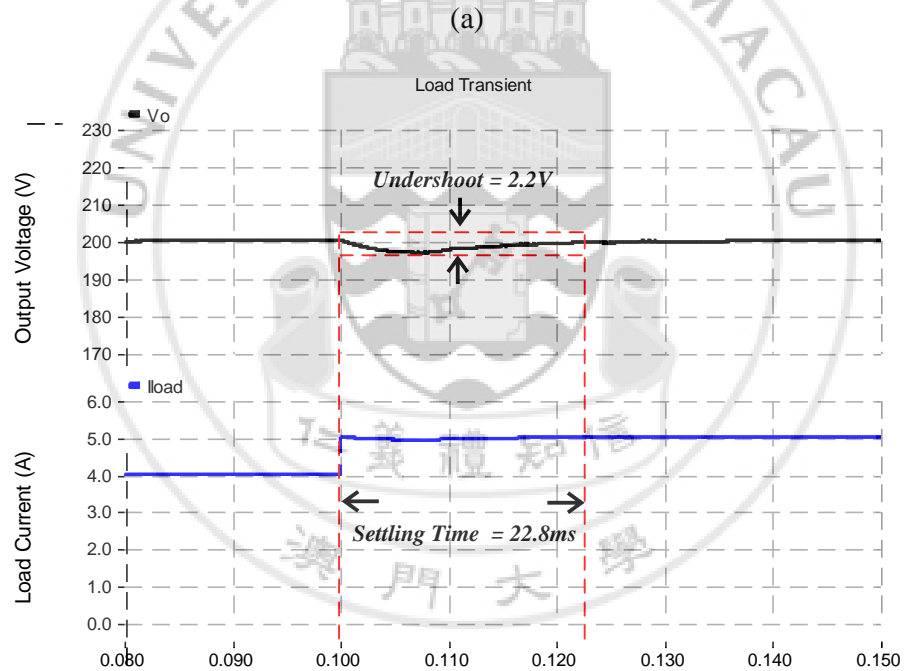can be test during the experiment. As the load increase, steady state error appeared since the controller is stilling under optimization.

Due to the equipment limitation, load transient from 6A to 2A cannot be test due to the equipment limitation. Load box be used will create a gap period to release the energy when the load current suddenly change from high load to low load.
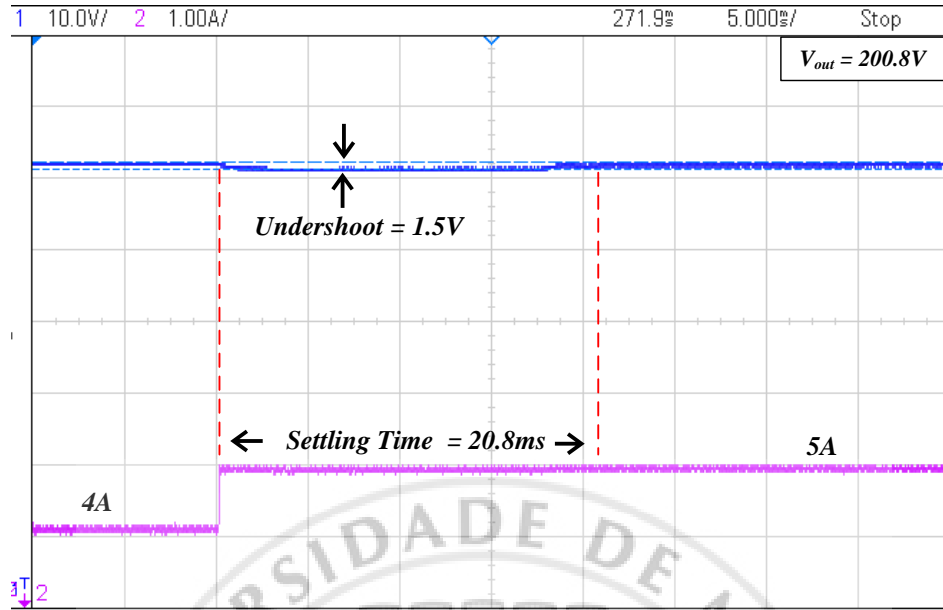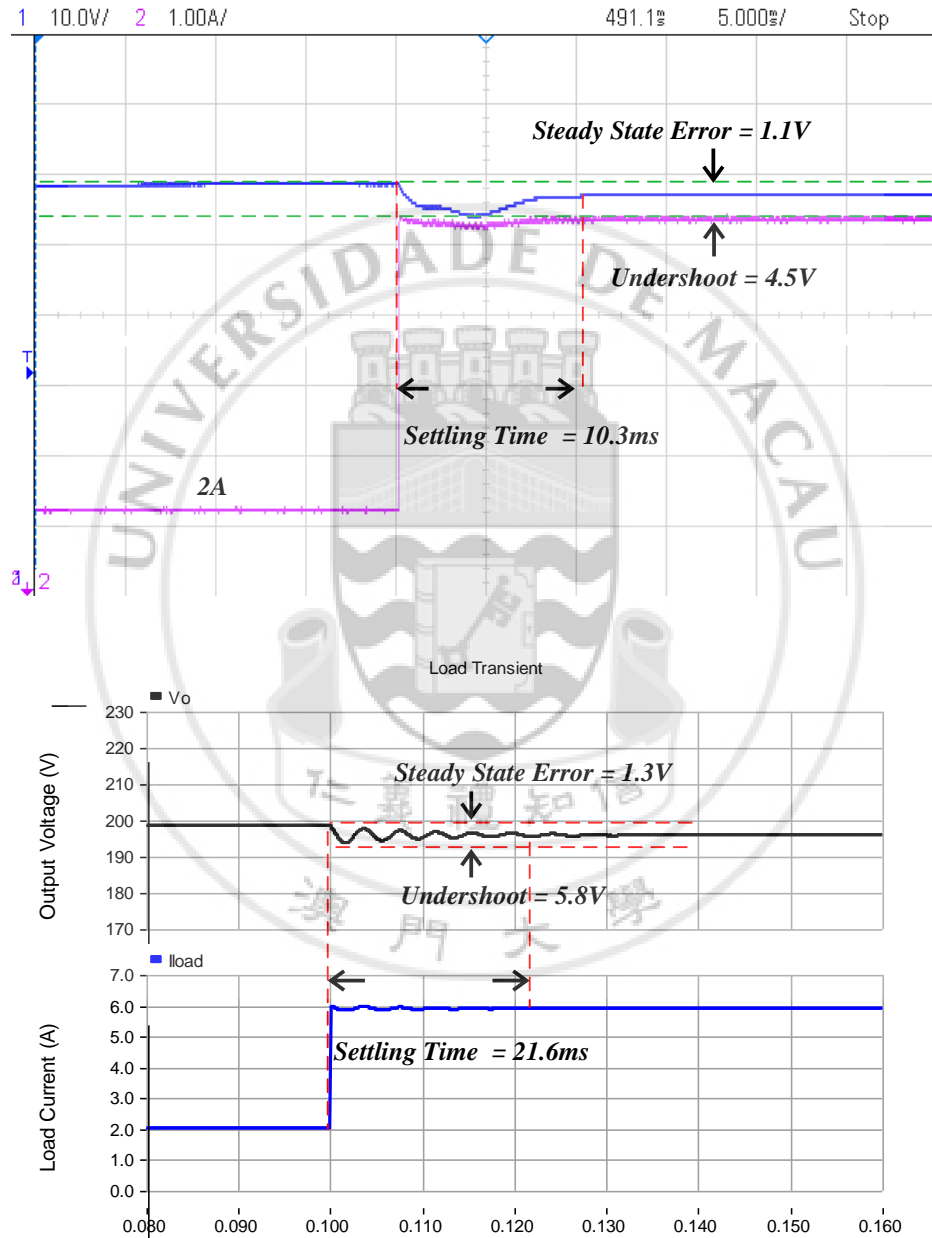

Figure 5.3.4 (a) Experiment and (b) Simulation result of close-loop load transient when load change from 2A to 6A

For more specific, figure 5.3.5 shows the load regulation for input from 120V – 140V and output from 180V – 200V under CCM. For current parameters, proposed KY converter already shows its ability of follow the reference setting by close loop control in CCM. Moreover, figure 5.3.6 and figure 5.3.7 depicts converter's efficiency versus the load current in CCM on simulation and experiment.

(a)   (b)

Figure 5.3.5 Load regulations for input of 120V – 140V and output of 180V – 200V from (a) Experiment; (b) Simulation

(a)   (b)

Figure 5.3.6 Efficiency of KY converter when L=220μH from

(a) Experiment and (b) Simulation

(a)   (b)
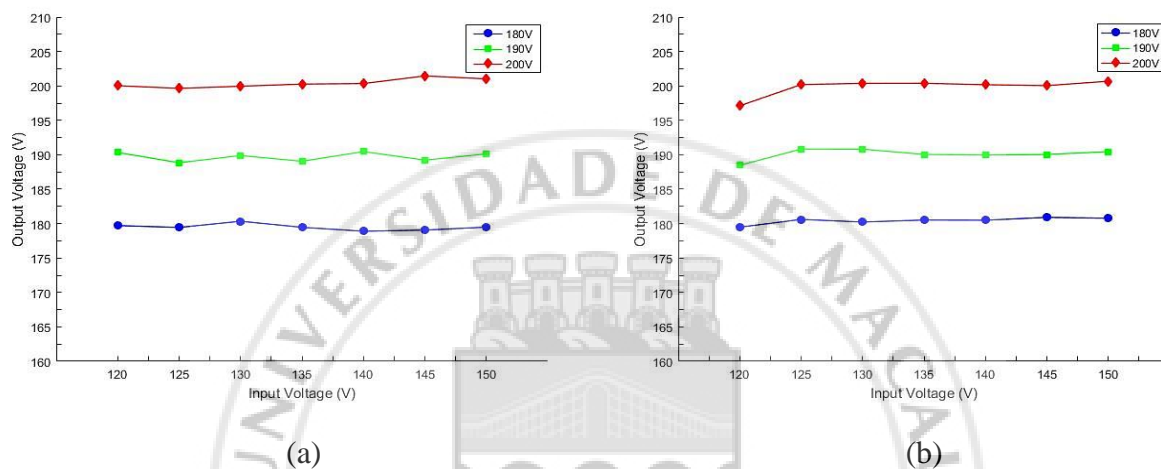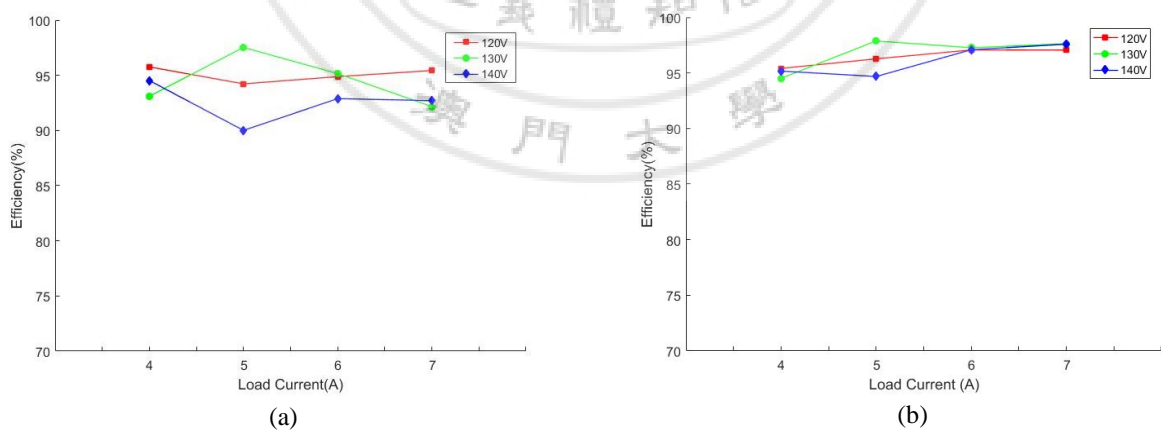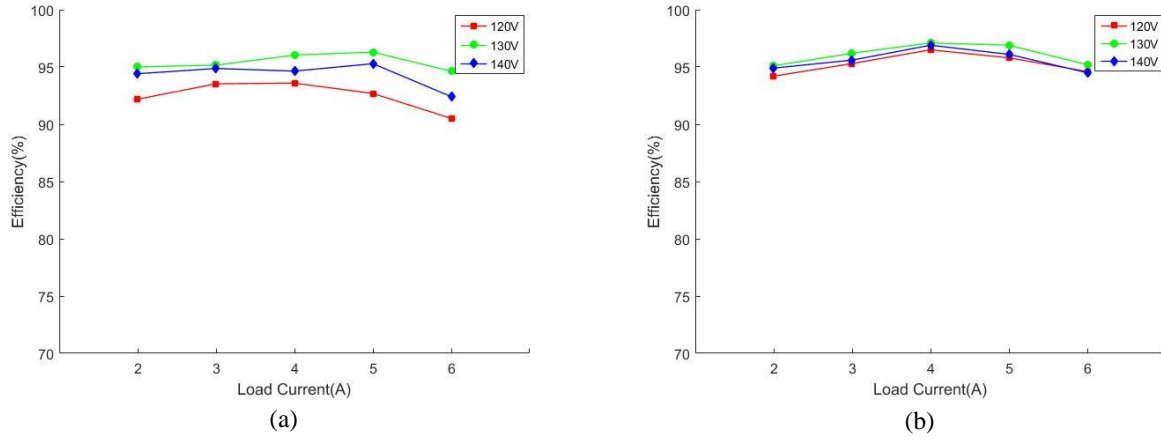
Figure 5.3.6 Efficiency of KY converter when L=500μH from

(a) Experiment and (b) Simulation

5.4 SUMMARY

In this chapter, simulation and experimental result of KY converter in different condition is given. PSCAD/EMTDC had been used for simulation, experiment is based on the hardware be introduced in chapter 4. From the experimental results of KY converter under CCM, proposed system is capable for maintain the output voltage around setting reference. For realization of PID control, P-only controller had been used for the experiment results shown in this chapter. Up to now, system is still under optimization for enhance performance and operation in DCM.

During the experiment the converter efficiency can be up to 97.5% (L=220μH, I_{load}=5A) for input and output voltage is 130V, 200V, respectively. As reference, [5.1]-[5.4] shows the result of other works on DC-DC boost converter in similar usage or claimed application as the proposed KY converter.

	[5.1]	[5.2]	[5.3]	[5.4]	This work
Input voltage (V)	48	48	65	48-75	130
Output voltage (V)	380	380	150	380	200
Switching frequency (KHz)	50	50	10	100	15
L (mH)	0.11	0.052	8	-	0.5
C (mF)	0.12	0.47	4.7	-	1
Cb (mF)	-	-	-	-	1
Load transient step (A)	-	2-3*	-	-	2-6
Vo undershoot / overshoot (V)	-	10*	-	-	2.3
Settling time undershoot / overshoot (ms)	--	100*	-		25
Maximum output Voltage Ripple level (%)		5*	-	-	0.5
Maximum Output Power (W)	3,500	200	-	1,000	1,200
Maximum efficiency (%)	94.65	90.1	93	90.5-92.3	97.5

*: Estimate by experimental result

Table 5.2 Performance comparison between the other works on DC-DC boost converter and the proposed KY converter

CHAPTER 6: CONCLUSION AND FUTURE WORK

6.1 CONCLUSION

A dc-dc converter called KY converter is proposed in this project. As a step-up converter which is capable to generate output voltage as twice as input in maximal, it is supposed to be used for boost up a 130V input from PV panel into 200V. By further connected with a DC/AC inverter, it allows the come from PV panel be directly injected into a 110V/3 phase power grid.

In this project, theoretical study and simulation analysis by PSCAD/EMTDC on KY converter has been done. After the correctness of theory had been verified, a hardware circuit was built up based on the theoretical design. Among the hardware, digital signal processor TMS320F2812 is used for realized PID control function and related switching logics for KY converter. Experimental was conducted by using a DC power supply and variable load box. From the experimental result of KY converter in continuous conduction mode, its efficiency is up to 97.5% for 5A load condition.

6.2 FUTURE WORK

Currently, proposed KY converter is still under conditioning for optimum performance. Effort in the future will be focused on:

- Enable proper operation of KY converter in discontinuous conduction mode;
- Achieve optimum performance by PID controller;
- Try to conduct experiment with PV panel as input and DC/AC inverter connected to load as claimed in the target application

REFERENCE

CHAPTER 1

[1.1]   "Global Power Electronics Market Size, Share, Development, Growth and Demand Forecast to 2022," P&S Market Research, Oct. 2016.

[1.2]   "Inverter Technology Trends & Market Expectations," Yole Development, Nov. 18, 2014.

[1.3]   "Inverter Market Trends 2013 - 2020 and Major Technology Changes," Yole Development, Feb. 2013

[1.4]   M. H. Rashid, Power electronics: Circuits, devices & applications, 4th ed. Boston: Prentice Hall, 2013

[1.5]   N. Mohan, First Course on Power Electronics, 1st ed. Hoboken, N.J.: Wiley, 2011.

[1.6]   Power Factor Correction Handbook, 2nd ed. Literature Distribution Center for ON Semiconductor, 2014.

[1.7]   K. I. Hwu and Y. T. Yau, "KY Converter and Its Derivatives," in *IEEE Transactions on Power Electronics*, vol. 24, no. 1, pp. 128-137, Jan. 2009

[1.8]   G. R. C. Mouli, J. H. Schijffelen, P. Bauer, and M. Zeman, "Design and Comparison of a 10-kW Interleaved Boost Converter for PV Application Using Si and SiC Devices," IEEE Journal of Emerging and Selected Topics in Power Electronics, vol. 5, pp. 610-623, 2017

[1.9]   M. Forouzesh, Y. P. Siwakoti, S. A. Gorji, F. Blaabjerg, and B. Lehman, "Step-Up DC DC Converters: A Comprehensive Review of Voltage Boosting Techniques, Topologies, and Applications," *IEEE Transactions on Power Electronics,* vol. PP, pp. 1-1, 2017.

[1.10]   Mitsubishi Electric, PV-MLE280HD2 datasheet, Jun. 2016

CHAPTER 2

[2.1]   K. I. Hwu and Y. T. Yau, "KY Converter and Its Derivatives," in IEEE Transactions on Power Electronics, vol. 24, no. 1, pp. 128-137, Jan. 2009

[2.2]   N. Mohan, First Course on Power Electronics, 1st ed. Hoboken, N.J.: Wiley, 2011.

[2.3]   F. Wang, Y. Zhang and X. Ma, "Small signal transfer functions modeling and analysis for open loop KY converter", in 2013 IEEE International Symposium on Industrial Electronics, 2013.

[2.4]   Vorperian, V., 'Simplified analysis of PWM converters using model of PWM switch. II. Discontinuous conduction mode', <u>IEEE Trans. Aerosp. Electron. Syst.,</u> May 1990, 26, (3), pp. 497–505, doi: 10.1109/7.106127

CHAPTER 3

[3.1]   "Stability analysis of switched DC-DC boost converter for integrated circuits" Rochester, New York

[3.2]   M. Kazimierczuk, *Pulse-width modulated DC-DC power converters*, 1st ed. Wiley, 2008.

[3.3]   C. Ka-Fai, L. Chi-Seng, Z. Wen-Liang, Z. Wen-Ming, S. Sai-Weng, and W. Man-Chung, "Generalized Type III controller design interface for DC-DC converters," in *TENCON 2015 - 2015 IEEE Region 10 Conference*, 2015, pp. 1-6.

CHAPTER 4

[4.1]   Mitsubishi Electric, "Mitsubishi Intelligent Power Modules," PM300DSA060 datasheet, Sep. 1998

[4.2]   LEM, "Current Transducer LA55-P", datasheet, Jun. 2015

[4.3]   LEM, "Voltage Transducer LV 25-400", datasheet, Mar. 2014

[4.4]   Texas Instruments, "OP07x Precision Operational Amplifiers," OP07 datasheet, Oct. 1983 [Revised Nov. 2014]

[4.5]   Texas Instruments, "TMS320F2812 Digital Signal Processor Data Manual", Apr.2001 [Revised May. 2012]

[4.6]   Texas Instruments, "REF50xx Data Manual", Jun.2007 [Revised Jun. 2016]

[4.7]   C. L. Phillips and R. D. Harbor, Feedback Control Systems, Prentice-Hall, Inc. , New Jersey, 1996

CHAPTER 5

[5.1]   Tseng, K. C., et al. (2017). "High Step-Up Interleaved Boost Converter for Distributed Generation Using Renewable and Alternative Power Sources." <u>IEEE Journal of Emerging and Selected Topics in Power Electronics</u> 5(2): 713-722.

[5.2]   Chen, Y. M., et al. (2013). "A High Step-Up Three-Port DC-DC Converter for Stand-Alone PV/Battery Power Systems." <u>IEEE Transactions on Power Electronics</u> 28(11): 5049-5062.

[5.3]   Bratcu, A. I., et al. (2011). "Cascaded DC-DC Converter Photovoltaic Systems: Power Optimization Issues." <u>IEEE Transactions on Industrial Electronics</u> 58(2): 403-411.

[5.4]   Qun, Z. and F. C. Lee (2003). "High-efficiency, high step-up DC-DC converters." <u>IEEE Transactions on Power Electronics</u> 18(1): 65-73.